IEEE Access
Multidisciplinary | Rapid Review | Open Access Journal

Received December 24, 2019, accepted January 6, 2020, date of publication January 9, 2020, date of current version January 21, 2020.

Digital Object Identifier 10.1109/ACCESS.2020.2965250

Residential Community Load Management Based on Optimal Design of Standalone HRES With Model Predictive Control

ESSAM A. AL-AMMAR[1], (Senior Member, IEEE), HABIB UR RAHMAN HABIB[2,3], KOTB M. KOTB[4,5], SHAORONG WANG[2], WONSUK KO[1], MAHMOUD F. ELMORSHEDY[2,4], (Student Member, IEEE), AND ASAD WAQAR[6]

[1]Department of Electrical Engineering, College of Engineering, King Saud University, Riyadh 11421, Saudi Arabia
[2]School of Electrical and Electronics Engineering, Huazhong University of Science and Technology, Wuhan 430074, China
[3]Department of Electrical Engineering, Faculty of Electrical and Electronics Engineering, University of Engineering and Technology Taxila, Taxila 47050, Pakistan
[4]Electrical Power and Machines Engineering Department, Faculty of Engineering, Tanta University, Tanta 31512, Egypt
[5]Electric Power Department, Faculty of Engineering and Informatics, Budapest University of Technology and Economics, 1111 Budapest, Hungary
[6]Department of Electrical Engineering, Bahria University, Islamabad 44230, Pakistan

Corresponding author: Habib Ur Rahman Habib (hr_habib@hust.edu.cn)

This work was supported by the Architecture and Urban Development Research Program funded by the Ministry of Land, Infrastructure, and Transport of the Korean Government under Grant 19AUDP-B099686-02.

ABSTRACT Microgrids being an important entity in the distribution system, and to get their full advantages by incorporating maximum distributed generation, standalone hybrid renewable energy systems (HRESs), being environmentally-safe and economically-efficient, are considered as the promising solution to electrify remote areas where the grid power is not available. In this work, a techno-economic investigation with an optimal design of HRES is presented to fulfill the domestic electricity need for a residential area of the Sherani district in the Province of Baluchistan, Pakistan. Nine case studies based on PV/wind/diesel/battery are analyzed based on net present cost (NPC), cost of energy (COE), and emission to decide the feasible solution. HOMER tool is utilized to accomplish modeling and simulation for economic analysis and optimal sizing. Simulation results demonstrated that HRES with PV-wind-battery is the most viable option for the specified area, and the optimal sizing of components are also obtained with $ 28,620 NPC and $ 0.311/kWh COE which shows 81.65 % reduction in cost and 100 % preserving in toxic emission while fulfilling 100 % energy demand with 67.3 % of excess energy. Furthermore, MATLAB/Simulink modeling for the optimally designed system is built for technical analysis while its effectiveness is proved by keeping dc and ac buses voltage constant, safe operating range of battery state of charge (SOC) with active power balance between HRES components, as well as efficient ac voltage quality, regardless of generation disturbances and load fluctuations. The output signal has total harmonic distortion (THD) of 0.30 % as compared to 5.44 % with the conventional control scheme. The novelty lies in the sequential application of both HOMER and MATLAB simulations of the proposed HRES model and validation of the proposition for the studied area; by using and implementing model predictive control (MPC) of a reconfigurable inverter.

INDEX TERMS Distributed power generation, energy management, finite control set model predictive control (FCS-MPC), design optimization, microgrids, dc-ac power converters, voltage control, energy conversion, energy resources, solar energy, wind energy, energy storage, maximum power point tracker (MPPT).

NOMENCLATURE

ABBREVIATIONS

TNPC	Total net present cost
VSI	Voltage source inverter
LCOE	Levelized cost of energy
IGBT	Integrated gate bipolar transistor
HRES	Hybrid renewable energy system
DERs	Distributed energy resources
IC	Incremental conductance
THD	Total harmonic distortion

The associate editor coordinating the review of this manuscript and approving it for publication was Tao Wang.

WT	Wind turbines
PV	Photovoltaic
DG	Diesel generator
HESS	Hybrid energy storage system
SC	Supercapacitor
MHT	Micro hydro turbine
BGG	Biogas generator
BM	Biomass
NGG	Natural gas generator
FC	Fuel cell
DSS	Discrete state-space
RES	Renewable energy source
AEDB	Alternative energy development board
COE	Cost of energy
MG	Microgrid
NPV	Net present value
GHG	Greenhouse gas
RERs	Renewable energy resources
MPC	Model predictive control
FCS	Finite control set
SOC	State of charge
PSO	Particle swarm optimization
PID	Proportional integral derivative
PPIB	Private power and infrastructure board
BSS	Battery storage system
PWM	Pulse width modulation
MFO	Moth-flame optimization
ANN	Artificial neural network
GWO	Grey-wolf optimization
WCA	Water cycle algorithm
ANFMD	Adaptive neuro-fuzzy modified dragonfly algorithm
GA	Genetic algorithm
FLC	Fuzzy logic controller
LCC	Life cycle cost
DOD	Depth of discharge
PMS	Power management strategy
PMSG	Permanent magnet synchronous generator
PE	Power electronic
EMU	Energy management unit
PFC	Power flow control
NREL	National Renewable Energy Laboratory
LLP	Loss of load probability
O&M	Operating and maintenance
RF	Renewable fraction
NEPRA	National electric power regulatory authority
MPPT	Maximum power point tracking
GENCO	Generation company
CD	Combined dispatch
LPSP	Loss of power supply possibility
TOPSIS	Technique for order preference by similarity to an ideal solution
WAPDA	Water and power development authority
DISCO	Distribution company
CC	Cycle charging
KESC	Karachi electric supply corporation
MRAS	Model reference adaptive system
SEPIC	Single ended primary inductance converter
LF	Load following
NTDC	National transmission and dispatch company
GCC	Gulf cooperation council

PARAMETERS, CONSTANTS, VARIABLES, AND FUNCTIONS

P_{charge}^{max}	maximum battery charging power
ρ	Air density
$P_{discharge}^{max}$	maximum battery discharging power
R	Rotor blade radius
P_{bat}	Battery rated power
v_w	Wind speed
N	System lifetime (yr)
V_{Bat}	Battery nominal voltage
λ	Blade tip speed ratio
B	Exponential capacity
F_{DG}	Fuel consumption rate (L/h)
β	Pitch angle
CRF	Capital recovery factor
$P_{DG,n}$	Nominal power of DG (kW)
C_p	Power coefficient
$C_{t,ann}$	Total annual cost ($)
$P_{DG,g}$	Generated power of DG (kW)
k_g	Gear ratio of the gearbox
R_b	Battery internal resistance
$\mathrm{V_c}$	Capacitor voltage
ω_t	Wind turbine rotational speed
$E_{t,ann}$	Total annual served load (kWh/yr)
$\mathrm{I_L}$	Load current
ω_D	DFIG generator rotational speed
K	Polarization voltage
$\mathrm{V_G}$	Grid side load voltage vector
H_D	Inertia constant of the DFIG
η_B	Battery efficiency
$\mathrm{I_F}$	Inverter output current
C_{Bat}	Battery capacity
$\mathrm{R_F}$	Filter resistance
Ah_{Bat}	Battery ampere-hour
V_o	Open circuit voltage
$\mathrm{L_F}$	Filter inductance
Wh_{load}	Load watt-hour
I_b	Battery discharging current
P_c	Emission cost
V_{Bat}	Battery voltage
A	Exponential voltage
C_C	Carbon content in kg/kWh
Wh_{night}	Night watt-hour
D_{Bat}	Duty cycle
CO_{2W}	Carbon weight in tons
Wh_{day}	Day watt-hour
j	Real interest rate (%)
$ETRC$	*R*enewable cost in $/kWh
n_a	Number of autonomous days
P_{mec}	Mechanical power from the wind

I. INTRODUCTION

Globalization and inter-countries energy sharing are considered as the conceivable future for the globe. In the present time, a significant proportion of the world's population is still living in remote rural areas with almost no access to electricity. Around 17 % of the world population (1.2 billion) cannot use electricity [1] and almost 80 % are living in rural spots [2]. Meanwhile, about 2 billion population around the globe have no access to grid-based electricity according to the most recent statistics [3]. Mostly, these peoples live in remote areas with no access to the national grid. According to [1], biomass is being used by around 3 billion worldwide habitats for cooking, heating and lighting purpose and resulted in 3.1 million premature deaths due to air pollution with incomplete biomass combustion. This is highlighted as the main reason for cramping the economic and social development of such communities in developing countries like Pakistan. Moreover, greenhouse gas (GHG) emissions are produced from many sources as shown in Fig. 1 in which it is noted that the dominant sector of producing these emissions is the energy sector through the conventional ways of energy production, while residential buildings indirectly produce the largest proportion of CO2 [4].

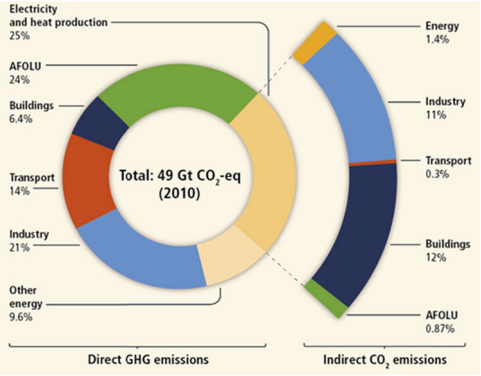

FIGURE 1. Sources of CO_2 by economic sector [5].

Conventional energy sources (CESs) cannot meet the day after day growth in energy demand due to their expensive capital cost, limitations of its fuel and the infeasibility of grid extensions due to geographical locations. Furthermore, as mentioned, CESs are the major contributor to greenhouse gas (GHG) emissions and the most severe threat to the environment and human health. Due to what has been mentioned, establishing small-scale grids (microgrids) is considered a shining solution to face most of the above-mentioned obstacles. Renewable energy resources (RERs) are the more feasible option to tackle all modern global warming and depleting fuel issues. These RERs (e.g. PV, wind turbines, fuel cells) can be easily integrated with each other in different microgrid (MG) configurations for electrification of remote and urban areas. The various hybrid configurations of RERs are adopted in literature and are considered as the most cost-effective, and environmentally friendly. However, its intermittent nature is considered as the main drawback which needs to be handled carefully with efficient energy management and control (EMCS) algorithms. Among the different control techniques that can be used to achieve the EMCS, Model Predictive Control (MPC) is utilized because of the reason that this algorithm is mainly classified as one of the most powerful artificial intelligence and non-linear programming approaches.

Due to the merits of MPC in addressing the systematic processing of constrained multivariable, it is well developed to handle the issues of power systems and power plants [6]. Hierarchical and distributed MPC is more efficient for handling large and complex power system problems through future prediction of control actions. Finite control set MPC (FCS-MPC) is the most frequently used among MPC controls due to its simplicity and high accuracy [7]. MPC is used in various applications including load frequency control for dynamic performance improvement under various disturbances and many applications in electrical drives (speed/position/torque control, torque ripple reduction, field-oriented control) [8]. VSI with LC filters is widely used in power supplies for high-quality output, which is also the future application in an embedded network of electrical aircraft [9].

Currently, renewable energy share worldwide is only 11 % while it is expected to increase by 60 % in 2070. The global capacity of wind and solar photovoltaic (PV) is increased to 514.8 GW and 399.6 GW respectively [6]. Fig. 2 shows the global trend for investment in the renewable energy sector. About the GCC countries [10], RERs penetration into the existing grid is an economically viable option for diversifying electricity mix and creating an avenue. Multi-directional power flow with a wide distribution system is the possible future of power grids in GCC states. Solar energy is going to be more competitive in all GCC regions and hence private firms would play their role in this regard. Proper deployment of new technologies (i.e. smart grid and smart cities) would be the economic growth factor with more revenue as well as the political stability of GCC countries with neighbors. The most feasible GCC regions for technology implementation are UAE, KSA, and Kuwait [10].

Pakistan is facing a severe problem of energy shortage and this shortfall is increasing with each passing day. Over 51 million peoples in Pakistan are still living with off-grid access to electricity [11]. Pakistan has initiated different projects in all provinces to curb the energy shortage problem. Potential areas for wind power projects include four sites in Punjab, twenty areas in Sindh, 25 points in Khyber Pakhtunkhwa, 23 sites in Baluchistan, two in FATA, three in Azad Jammu and Kashmir, 11 in Gilgit Baltistan [12]. World Bank has installed MHP weather stations in nine cities with consideration of five family members in one household [13]. In Pakistan, key points of national power policy 2013 include load shedding elimination, decreasing transmission and distribution losses from 23–25 % to 16 %, increasing revenue from 85 % to 95 % and time reduction for decision making. Power policy 2015 focused on private

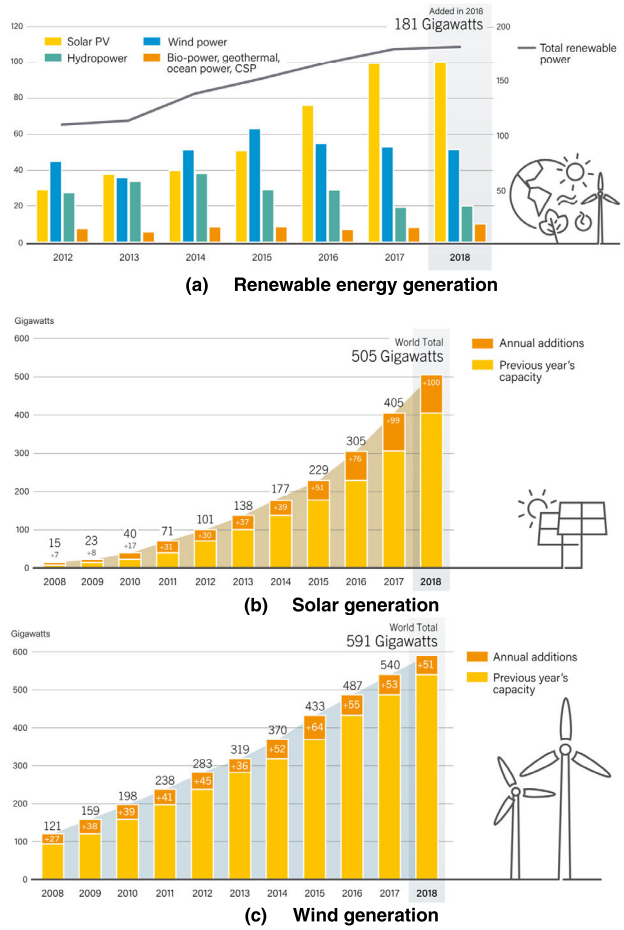

FIGURE 2. Global trends of renewables [16].

investment in the energy sector for sufficient power generation capacity, least COE, priority of indigenous resources' use, facilitating all stakeholders and safeguarding the environment [14].

Pakistan is bestowed with a high potential for RERs (solar and wind). These RERs are not comprehensively explored so far. The country is dependent mainly on thermal, hydro and nuclear energy, which creates acute energy shortage problems nationwide especially in rural areas where grid power is not available. Remote area electrification is normally carried out by expensive grid extension, small hydro and diesel power plants, which have a severe impact on health as well as environment. It is expected to achieve a target of 5 % renewable energy mix until 2030, currently, there is no significant penetration of renewable energy. Renewable energy activity in Pakistan is considered very promising to be exploited, the daily solar radiation ranges from 4.68 kWh/m^2/day to 5.54 kWh/m^2/day while the annual global irradiance range lies between 1900-2200 kWh/m^2. Additionally, about 346 GW wind potential is also available. As this study aims at the electrification of one of the Pakistani rural communities, one household maximum load is considered to be 21.57 kWh which is also shown in Table 5 while energy ranges for domestic community load are shown in Table 1 [15].

TABLE 1. Energy Generation capacity [15].

Range	Capacity	Type of load demand
Large-scale	Greater than 100 kW	Territory loads
Medium-scale	From 5 kW to100 kW	Grid-isolated community
Small-scale	Less than 5 kW	Remotely located houses

The organization of the remaining paper is presented as follows; a literature summary and comprehensive comparative analysis are established and described in section II along with the main objectives, scope, and significance of the proposed scheme. Section III presents the detailed system description which includes feasibility study (site/resources selection, load estimation), and modeling of HRES components (PV, WT, DG, battery, and power converter). Detailed discussion on techno-economic analysis using HOMER is planned in section IV which includes the optimal design objective and constraints supported with a detailed flow chart. Section V investigates the technical aspects using converters controllers in MATLAB/Simulink for the most optimal plan obtained from section IV while section VI describes the simulation results with detailed discussion for the suggested model. Section VII compares and verifies the key results of the proposed model with literature studies along with the main findings. Finally, the conclusion is grasped in section VIII.

II. RESEARCH BACKGROUND SYNOPSIS

Several researchers emphasized the study of standalone HRES. Table 2. summarizes the addressed researches that investigated such kind of systems, such as the configuration of the HRES, the applied algorithms as well as the main objectives are presented. Table 3 shows a comprehensive study of the research methodologies of the literature in terms of their contribution and drawbacks. According to the performance rating for the suggested energy management and control of HRES, a comparison between suggested work and presented literature is shown in Table 4. Results show that most of the literature investigated PI-based control but thorough investigation on the basis of design optimization is not presented. The wind control unit in the current study includes an uncontrolled rectifier which is simple, and economical. Moreover, an uncontrolled rectifier works without IGBTs and there is no need for additional controllers for control signals and thereby reducing the complexity and system cost. Most of the published literature was not thoroughly analyzed by considering wind and PV MPPT, uncontrolled wind rectifier, battery controller for regulating dc voltage, THD analysis, comparison of PI and FCS-MPVC for inverter control.

Most of the addressed literature studies have been solely concentrated on either design optimization of HRES or energy management system (EMS). In this work, the optimal design of HRES with the most suitable and advanced EMS approach is proposed. First, the detailed techno-economic analysis with multiple hybrid scenarios for diesel, solar photovoltaic (PV), wind, battery, and converter are

TABLE 2. Summary of the Literature review.

Ref-year	Construction/type	Main Concerns	Applied Algorithms	Location
[17]-2016	PV-diesel-battery/Isolated	NPV, emission, loss of load probability (LLP)	PSO by Matlab/Simulink	Algeria
[18]-2012	PV-wind-battery/Isolated	Sizing the wind and PV components along with storage capacity	Proposed Simple Sizing Algorithm by Matlab/Simulink	China
[19]-2015	PV-wind-diesel-battery/Isolated	Optimum configurations, COE, NPC, and greenhouse gas (GHG) emission	HOMER	Egypt
[20]-2015	PV-wind-diesel-battery/Isolated	Economically feasible and environmentally non-toxic investigation of net-zero HRES	HOMER	Egypt
[21]-2016	PV-wind-diesel-battery/Isolated	Sizing optimization, total annual cost, LPSP, and diesel fuel cost requirement	GA-Teaching Learning-Based Optimization- Clonal selection algorithm by Matlab/Simulink	South Korea
[22]-2017	PV-wind-diesel-battery/Isolated	Identifying the best compromise configuration of hybrid energy systems	HOMER	China
[23]-2018	PV-wind-battery/Isolated	Modeling and control of hybrid systems using Quasi Z-source inverter	PV-MPPT by Matlab/Simulink	---
[24]-2019	PV-battery/Isolated	Energy management scheme with battery life span enhancement	ANN by Matlab/Simulink	---
[25]-2019	PV-wind-diesel-battery/Isolated	Optimal sizing and costs optimization	Grey-wolf optimizer (GFO) by Matlab/Simulink	Nigeria
[26]-2019	PV-wind-battery/-	Practical realization of hybrid systems-Enhancement of the MPPT techniques for the wind systems	ant colony optimization (ACO)-MPPT-FLC by Matlab/Simulink	India
[27]-2019	Different Hybrid Energy Systems/-	Reliability indices, LPSP, LLP	(PSO, GA, ANN) by Matlab/Simulink	---
[28]-2019	PV-wind-battery/Isolated	Mitigating the disharmony between load/generation balance, cost optimization, saturation	Proposed sizing methodology by Matlab/Simulink	China
[29]-2019	PV-biogas-hydro-battery/-	Obtaining the techno-economic optimal design, loss of load probability	WCA, MFO	India
[30]-2019	PV-wind/Isolated	Feasibility study including economic aspects	HOMER	Ethiopia
[15]-2019	PV-wind-fuel cell/Isolated	System optimization and EMS, LPSP	The proposed methodology by Matlab/Simulink	---
[31]-2019	PV-wind-battery/Isolated	Feasibility study of hybrid systems including economic aspects	PSO by Matlab/Simulink	India
[32]-2019	PV-fuel cell/Isolated	Irrigation site fully energization from RERs, the effect of combining consumptions	The proposed methodology by Matlab/Simulink	Spain
[33]-2019	PV-diesel-battery/Isolated	SOC management strategy- load following and cycle charging strategies	FLC by Matlab/Simulink	---
[34]-2019	PV-wind/Isolated	The economic investigation, system performance comparisons	MPC by Matlab/Simulink	---
[35]-2019	PV-fuel cell-ultra capacitor/Isolated	Energy management strategy, improve power security, efficient production of electricity without interruption	The proposed methodology by Matlab/Simulink	Tunisia
[36]-2019	PV-diesel-battery/Isolated	Benefits of low social and private costs with the combined use of PV based electrical-thermal systems	Bi-level optimization	China
[10]-2019	Wind Farms/Isolated	Techno-economic feasibility analysis for 15 MW wind farms at two sites with a significant reduction of COE.	HOMER	Saudi Arabia
[37]-2019	PV system/Isolated	Most feasible locations for a PV system to replace natural gas/diesel with reduction of emission, COE, and NPC.	HOMER	Oman

TABLE 3. Comprehensive analysis of literature study.

Ref	Contribution	Critical Analysis
[1]	• PV-WT-MHT-DG-battery system with nine HRES configurations is proposed for fulfilling remote area electricity demand in Southern Cameroons for a community load (residential) of 100 kWh/d. • PV-DG-MHT-battery is the most viable option with COE of $ 0.443/kWh. • Sensitivity analysis based on streamflow, interest range, fuel consumption, and PV price is analyzed.	• Study location (Wum) has inadequate wind speed (about 2.5 m/s max) which is not feasible for wind generation. • The proper control design for the optimal HRES is missing.
[2]	• PV-WT-battery based three HRES configurations are proposed for rural electrification in Yamunanagar district of the State of Haryana, India for a community load (residential & agricultural) of 151.65 kWh/d. • PV-WT-battery is the most viable option with COE of $ 0.288/kWh. • Technical analysis is conducted by developing control and SOC management scheme of the most optimal configuration plan. PI control is implemented for inverter control.	• With PI control, load voltage quality is very low due to high ripples (Fig. 26) with a THD of 2.37 %. • The proposed PV system (121 kW) is not implemented during the power-sharing of different components (Figs. 22, 27). • A dc bus voltage is distorted between 2-6 sec (Fig. 19) which shows the inadequate tuning of the PI controller.
[6]	• Hierarchical control using distributed MPC is applied for standalone PV-WT-battery for dc bus only.	• Inverter control for efficient load voltage quality at the ac bus of HRES is not implemented.
[7]	• Senseless MPC of the AFE rectifier is proposed. • Two self-created problems due to the proposed model scheme namely current derivatives and inductance parameter estimation are addressed by using filters and MRAS observer.	• External disturbance by including real-time sources (PV, wind, etc.) and variable load is not comprehensively included. • The system is tested for a very low dc bus voltage.
[18]	• A simple algorithm for optimal PV-WT-battery standalone system to minimize life cycle cost with invariant SOC criteria is applied for the Zhoushan islands of China (office load). • By keeping SOC constant during each time instant, the number of WT and PV are changed based on the load requirement with 65 % DOD and 60 % initial SOC.	• No comparative analysis of the proposed algorithm with other schemes is carried out.
[22]	• Weighted sum method for decision making to find the best trade-off HRES plan based on PV-WT-DG-battery is proposed for remote Yongxing island of China. • Sensitivity analysis based on PV/WT/fuel cost is performed for the viable option based on practical, environmental, and economic aspects.	• The effectiveness of the proposed method is not analyzed.
[23]	• Hybrid PV-WT MG using a quasi Z-source interlinking inverter and proposed PV-MPPT (P&O) controller using the dc-dc SEPIC module are studied. • No filter is required with improved performance due to the incorporation of the suggested inverter. • The dSPACE hardware setup is implemented to validate the suggested model.	• Wind MPPT is not modeled in the simulation. • The experiment is conducted for very low power ratings (150 W in Fig. 11) which is not feasible for practical applications. • No simulation results are shown for the proposed model. • Wind speed in the experiment is taken as 22 m/s (Fig. 11) which is impractical for real-time scenarios.
[24]	• PV-HESS standalone LVDC bus system (60V) with SOC management of HESS using ANN is implemented and tested experimentally. • The implemented strategy has effectively use SC energy. • PI controllers of HESS are optimized using the PSO algorithm.	• No WT based integrated system is considered. • Power level is very low (400 Wmax) which is impractical for real study cases.
[25]	• Standalone PV-WT-DG-battery system for 500 rural households with 493 kWh/d load is implemented for six zones in Nigeria. • The lowest COE of $ 0.658/kWh of optimal PV-DG-ESS system is obtained for the Maiduguri site of the northeast zone.	• Improper components selection is made during feasibility studies as WT cannot be considered for optimal zone due to low wind speed (3.52 m/s max). • No GHG emission is considered.
[26]	• PV-WT-battery standalone system with ACO based cuk controller as an efficient wind MPPT strategy compared to PSO is suggested with experiment (dSPACE) using FLC for the interlinking inverter to feed the ac load.	• A rapid charging method may reduce battery life without proper storage considerations. • No PV MPPT algorithm is suggested to extract maximum solar power. • The load voltage quality is poor (Fig. 8) and low power rating (200W max) in Fig. 7 is impractical.
[28]	• Out of 150 configurations for standalone PV-WT-battery, the WT-battery system is the most optimal plan for Jiuduansha island (ten households with 255 kWh/d load) in Shanghai China with COE of $ 0.187/kWh and 80% DOD. • Sensitivity analysis with wind energy, storage cost, and load variation is investigated.	• Details of the system performance tool which is used to conduct the analysis are not mentioned.
[32]	• Vineyard in Spain is chosen for 100 % renewables (PV-battery) for water purification and irrigation system. FCHEV is fed with hydrogen by using surplus energy.	• No economic considerations (NPC, COE, etc) are taken.
[33]	• Fuzzy based dispatch is shown as an efficient strategy for PV-DG-battery based residential electrification system as compared to LF and CC with COE of $ 0.194/kWh.	• The controllers for PV MPPT and dc bus voltage control is not analyzed. • Electrical load estimation along with site selection is not defined and practical data of PV irradiance and load profile is not considered in the study.
[38]	• An intelligent battery controller is suggested for the PV-WT-battery system during variable load and sources. • A conventional PI scheme is applied for the interlinking converter to regulated the load voltage. • IC method for PV MPPT is used to extract maximum solar power. • A battery management strategy is applied to optimize the charging/discharging.	• Poor load power quality is observed (Fig. 14). • Load voltage mismatch is high (Fig. 17) • No economic analysis is performed. • No explanation of dc bus voltage control is shown which is the primary goal of an intelligent battery controller. • High wind power transients show the ambiguity of the implemented WT model (Fig. 14). • No wind MPPT is analyzed in detail.

TABLE 3. *(Continued)* **Comprehensive analysis of literature study.**

[39]	• Smart battery life enhancement strategy is applied for a standalone PV-battery system to feed the rural community in Sarawak Malaysia with an overall reduction in battery cost by using actual solar irradiance and estimated load data. • Battery stresses are mitigated by analyzing frequent charging/discharging, high C-rate, and power surges by addressing current fluctuations and surge currents. • Li-ion and lead-acid batteries with SC are used in the HES plug-in module. • The proposed strategy is validated through a scaled prototype experiment.	• No dc voltage control analysis is carried out which is the sole purpose of a battery controller. • The inverter control strategy is not applied for efficient load voltage and power quality. • No economic analysis for the overall PV-batteries model is performed which is essential for feasibility.
[40]	• Off-grid rural electrification PV-DG-battery system with CD strategy is suggested for the Diyala district of Iraq with a daily load of 145 kWh/d. • Three dispatch strategies viz. LF, CC, CD are compared. • Sensitivity analysis viz. minimum SOC, time step, PV radiation, DG fuel cost, and load is analyzed. • Optimal configuration with CD strategy is proposed with COE of $ 0.210 /kWh.	• No control strategy is implemented for the optimal configuration plan (winning plan) which highlights technical aspects of the proposed system model.
[41]	• The standalone PV-WT-battery system for eight consumers in the Mostaganem of Algeria is studied with eight case studies of different consumer sectors of 8.63 MWh load. • Two storage configurations viz. battery and pump are used. • Bi-objectives viz. cost minimization and reliability enhancement are formulated by using GWO. • Emission is reduced without proposing any optimal configuration plan.	• No economic model with renewables is found. • The control methodology of the implemented hybrid system is not carried out for technical analysis.
[42]	• Standalone DGWT-battery system for a residential load of Quetta city of Baluchistan Pakistan with power management and control strategy using model predictive control. • The techno-economic analysis is carried out for the optimal configuration plan (WT-battery) with the minimization of NPC, COE, and emission. • Technical analysis with power management strategy of the winning plan is carried out with different converters controllers keeping in view the wind MPPT and SOC.	• PV is not incorporated for the analysis to highlight the possible renewable energy potential of the proposed area.
[43]	• PV-WT-BGG-battery system for urban electrification (residential/commercial/industrial) in Victoria City of Canada is proposed. • Three scenarios namely only NG, NG-RER, and RER only are taken to reduce NPC. • COE with PV-WT-BGG is reduced three times as compared to the PV-WT model and it is further reduced by incorporating NGG. • Sensitivity analysis based on the discount rate, PV/battery capital cost is carried out. COE is more sensitive to battery capital cost as compared to PV capital cost. • NPC and COE for residential/commercial/industrial loads are million $ 42.9/48.0/41.9 and $ 0.418/kWh, $ 0.399/kWh, $ 0.385/kWh respectively.	• No control strategy is applied for technical analysis of the most feasible configuration plan.
[44]	• PV-WT-DG-battery system is proposed for the New Borg EI Arab city of Egypt to feed the residential and industrial load with minimization of NPC, COE, and emission. • COE and NPC for the optimal configuration plan are $ 0.190/kWh and $ 1,684,118 respectively.	• Control strategy for the most optimal configuration plan (winning plan) is not implemented which is the validation of the technical analysis.
[45]	• Hybrid PV-WT-DG-battery system for six domestic sites in the south-south zone of Nigeria is presented by introducing TOPSIS multi-criteria decision methodology which considers different aspects viz. techno-economic, environmental, and social.	• Power management and control methodology for the most feasible system is not presented to highlight the control aspects of the proposed models.
	• The most optimal plan for three cities is PV-WT-DG-battery and PV-WT-battery remaining cities with COE ranges from $ 0.459-0.562/kWh with payback time from 3.7-5.4 years.	
[46]	• ANFMDA is applied to optimize the MG configuration (optimal energy management) in the first step followed by the load prediction which shows superior performance over three different algorithms. • Optimization is based on minimum fuel cost and load prediction focus on the minimization of annual fuel price, operation/replacement cost.	• Economic analysis based on NPC and COE is not performed. • No PV and WT detailed modeling are examined. • A control strategy for technical analysis is not considered.
[47]	• PV-DG-battery system is proposed to feed 20 houses load (47 kWh/d) in Saharan village located in the Tazrouk district of Tamanrasset province of Southern Algeria. • Sensitivity analysis based on load consumption, emission, LLP is analyzed. • PSO is found superior as compared to HOMER in terms of COE, more RF (PV), carbon emission	• No EM and control scheme is presented for the optimal plan.
[48]	• Grid-connected PV-WT system for Bandar Abbas city in Iran is proposed with four vertical axis wind turbines (VAWTs). • VAWTs are simple in structure and installation with different speed ranges and directions. Further, these are cheap to manufacture and easy for maintenance without the need for any supportive tower while less noise, as well as smaller sizes, are also the main attributes.	• Technical implementation of the suggested system with the feasible controllers along with modern online control techniques is not applied in this study. • Mathematical models with detailed analysis of VAWTs as well as the objective functions are not described.
[49]	• Iraqi rural village (30 houses with 19.846 kWh load) is electrified with off-grid PV-hydro-DG-battery as the most optimal configuration plan by keeping in view the low emission with only 6444 L diesel. • As compared to a single year with NPC and COE as $ 92381 and $ 0.0458/kWh respectively, the multi-year (20 years) analysis has reduced PV production by 9.1 %, increased diesel operation by 90.8 %, emission by 91.7 %, and server load by 8.8 % with NPC of $ 113201. • Sensitivity analysis based on water pipe losses, DG minimum load, battery efficiency, SOC value, capacity shortage, PV capital cost, and multi-year is applied.	• The control and energy management strategy for the optimal configuration plan is not implemented which can validate the model on technical grounds. • The suggested system is not good for multi-year analysis because of no benefit with various demerits mentioned before.
[50]	• MPC and GA are used for the PV-WT-biomass system for optimal dispatch with demand response using the experimental platform (LabDER). • Energy management and optimal controller selection with battery/hydrogen storage for the residential load are used to obtain minimum cost and computational burden with maximum RF.	• No controller for the converters of the suggested model is implemented by maintaining maximum power extraction from PV-Wind with the regulation of dc/ac bus voltages for better load power quality.
[10]	• PV-WT-battery based hybrid system is proposed for the mosque load (33.27 kWh/d) in Alaris town of Saudi Arabia. • The NPC and COE for the optimal configuration are $ 35449.35 and $ 0.226/kWh.	• No detailed modeling of the HRES components is investigated and the dispatch strategy with possible EMS/control scheme is not included.

TABLE 4. Comparative analysis of suggested methodology with the literature study.

Ref	Sizing Optimization	Wind MPPT control (Boost)	PV MPPT control	DC voltage control Analysis	SOC Control	Inverter Control (PI)	Inverter Control (MPC)	THD Analysis
[38]	No	Yes	Yes	No	Yes	Yes	No	Yes
[39]	No	No	Yes	-	Yes	No	No	No
[51]	Yes	No	No	No	No	No	No	No
[24]	No	No	Yes	-	Yes	No	No	No
[25]	Yes	No	No	No	No	No	No	No
[40]	Yes	No	No	No	Yes	No	No	No
[41]	Yes	No	No	No	No	No	No	No
[26]	Yes	Yes	No	Yes	No	Yes	No	No
[32]	Yes	No	No	No	Yes	No	No	No
[52]	Yes	No	Yes	Yes	No	Yes	No	No
[53]	Yes	No	No	No	No	No	No	No
[33]	Yes	No	No	No	Yes	No	No	No
[54]	Yes	No	No	No	No	Yes	No	No
[6]	No	No	No	No	Yes	No	No	No
[42]	Yes	Yes	No	Yes	Yes	Yes	Yes	Yes
Present	Yes	Yes	Yes	Yes	Yes	Yes	Yes	Yes

applied for the design optimization of HRES. The developed model is then utilized to fulfill the load demand of an islanded domestic area sited in Pakistan with the consideration of real demand profile and weather information. Second, MATLAB/Simulink® is used to develop a self-made simulation tool for the implementation of the suggested EMS. The optimized model is tested on the proposed EMS and the performance of the suggested model is improved for power quality, steady-state and transient stability with intermittent generation and fluctuating load demand.

Summarized points from the comprehensive literature review are:

- The HRES configurations are considered to be the most reliable and economically viable options with minimum GHG emissions. While multiple configurations are possible for any specific location based on load profile, resources data, and environmental conditions.
- The major focus of the literature is either on optimal sizing with economically viable configuration or on power management of HRES. Both features are not given much attention at the same time. According to the best of authors' understanding, the proposed strategy by handling optimal design and power management simultaneously for the PV-WT-Battery system using FCS-MPC with reconfigurable inverter for a standalone HRES is not investigated in the literature.

Based on the above-mentioned circumstances, the objectives and scope of the presented work are summarized as follows:

- To fulfill the drastic increase in electricity demand, the sample location of the Baluchistan province in Pakistan is investigated with the available energy resources including PV and wind.
- A unified and generic methodology for optimization of components size with power control and energy management for off-grid HRES is presented. The proposed methodology is endorsed with a real domestic case study for electrification in Pakistan.
- The optimal HRES scheme is obtained with the aid of feasibility study keeping in view the minimum cost and least emission. Minimum TNPC, LCOE, and improved model reliability are integrated as an objective function. HOMER® software is used for this purpose.
- Verification of a properly designed EMS is executed with the help of a self-made Simulink model in MATLAB® environment. The suggested EMS strategy is implemented with battery SOC to maintain load balance as well as dc bus voltage by keeping in view the battery SOC within the permissible limits, with maximum wind and PV power extraction while maintaining the ac bus voltage constant under fluctuating loads, and source disturbances (wind speed and solar irradiance).

MPC is the most preferable solution for complex control problems [55]. The advantages of the suggested FCS-MPC based model are listed as follows:

- The significant advantage of MPC management is simplicity while the concepts are very heuristic and intuitive in nature and easily understandable.
- The suggested MPC based EMS model is more proper for multi-variable systems and can be extended accordingly.
- The suggested EMS model is applicable for real on-line systems of non-linear nature.
- The proposed FCS-MPC methodology with a complete solution for optimal design with energy management and control for the proposed domestic site is not analyzed in the literature.
- The extension of the system with the proposed FCS-MPC controller is very easy ranging from domestic to commercial and agriculture loads.
- The proposed control strategy with FCS-MPC selects the optimal strategy by controlling the interaction and

constraints among different variables. Therefore, this strategy serves the purpose of economic benefits with the quick operation and predicts the dynamic behavior for linear as well as non-linear multivariable models.

- As compared to most widely used PI control, the suggested MPC based model can also be applied for grid-connected applications in addition to standalone systems during transient stability analysis.
- The settlement time for FCS-MPC control is less and is applied to minimize the errors and eliminate signal harmonics from the output voltage/current.
- The proposed control methodology does not need any modulation scheme and is applicable for variable switching frequency.
- The steady-state performance is better for all three reference frames with low design complexity and easy implementation of the resulting FCS-MPC controller in experimental studies.
- The current model based on PV-WT-DG-battery-converter is the improvement of the WT-DG-battery-converter model of [42] by incorporating a detailed analysis PV model.

III. SYSTEM DESCRIPTION

Pakistan is situated in South Asia with its 1046 km coastline alongside the Arabian Sea as well as the Gulf of Oman as shown in Fig. 3. Neighboring countries include Afghanistan and Iran on the west-side, India in the east-side, and the north-side is China. Geography includes the Thar Desert on the east-side while Himalayas, Hindu Kush and Pamir mountains on the north side. It was an ancient trade route between Asia and Europe with 796,095 square kilometer territory [56]–[58].

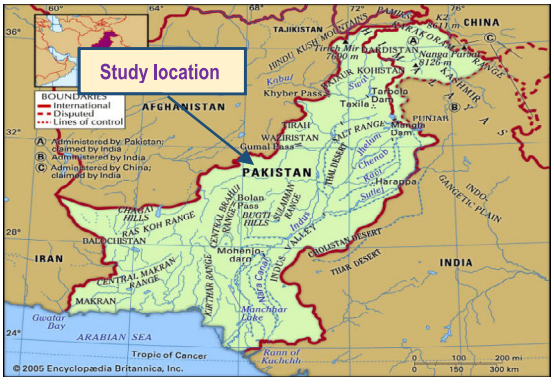

FIGURE 3. The case study location in Pakistan.

The power sector of Pakistan is operated by WAPDA as well as KESC. KESC rebranded as K-Electric has the responsibility of generation, transmission, and distribution of the electricity to Karachi city and neighboring localities while WAPDA has the responsibility to provide generated power to the rest of the country. Under the new institutional setup, NEPRA is an independent regulatory authority for ensuring a transparent, competitive and commercial based power market. WAPDA is further divided into four public sector GENCOs, ten DISCOs, and NTDC. PPIB is established to facilitate the power sector with private investment and is handling the development of renewable energy resources (RERs). PAEC (Pakistan Atomic Energy Commission) develops nuclear power [14].

A. SITE DESCRIPTION AND ENERGY RESOURCE ASSESSMENT

The suggested methodology of HRES design and control is employed for the rural area electrification of a domestic load which is located in the province of Baluchistan Pakistan as shown in Fig 3 where the utility grid availability is obsolete. The wind speed range in Baluchistan province is observed to be 4 to 9 m/s and 12.5 m/s at 10 m and 50 m hub height respectively [59]. The designated location has Latitude and longitude of 31 ° 31.4' N and 69 ° 56.3' E respectively as shown in Fig 4 with wind energy potential. While 4 kWh/m^2/day is the annual radiation as shown in Fig 5. A plenty of PV and wind generation is available in Pakistan with friendly climate conditions [60]. PV and wind data for the selected site are taken from NASA [61]. The average wind speed, PV irradiance, and temperature data are shown in Fig 6, Fig 7, and Fig 8 respectively with an average value of 5.62 m/s and 5.18 kWh/m^2/day respectively.

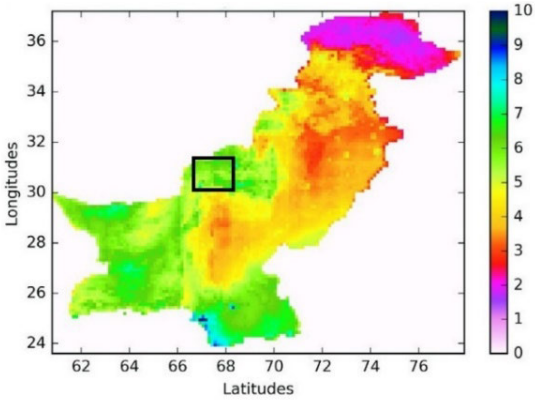

FIGURE 4. Wind power atlas in Pakistan.

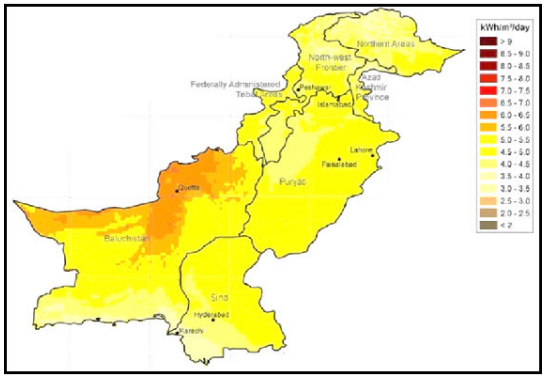

FIGURE 5. Solar power atlas in Pakistan.

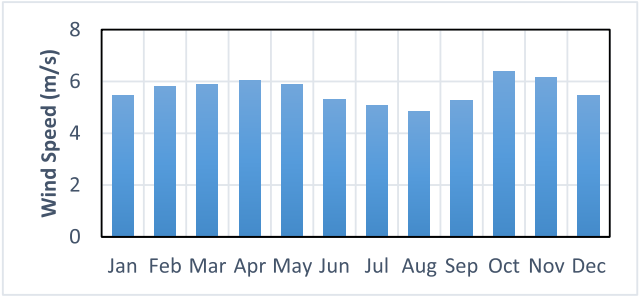

FIGURE 6. Monthly average wind speed in the studied location.

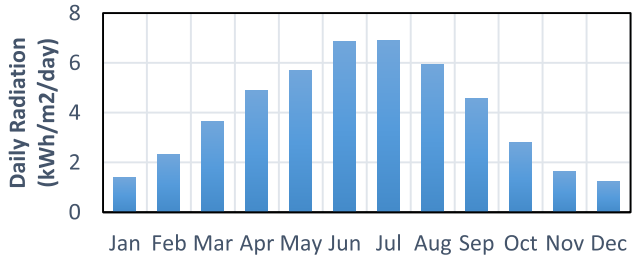

FIGURE 7. Monthly average Solar irradiance in the studied location.

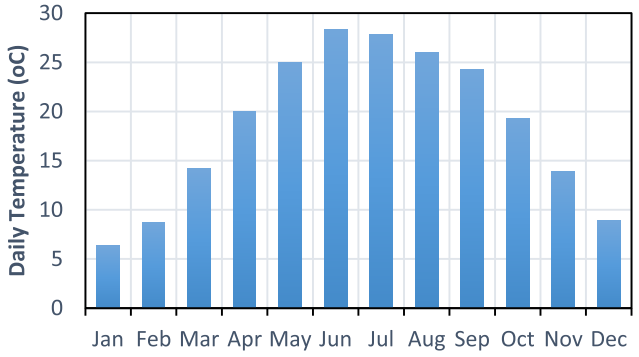

FIGURE 8. Monthly average temperature in the studied location.

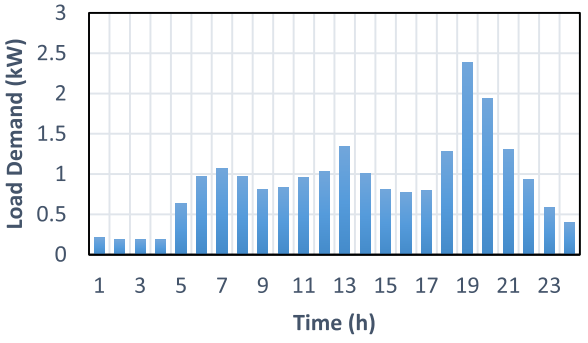

FIGURE 9. Daily load data of three households.

B. ELECTRIC LOAD ESTIMATION

In this study, the local survey for the load estimation of one household is carried out in the Sherani district of Baluchistan. The energy consumption activities of prime importance are shown in Table 5. The estimated load demand is 3.62 kW (peak value) while the annual utilization is 21.57 kWh/day. Fig 9 shows the load profile for three typical houses of the selected location.

TABLE 5. Calculation of Residential load.

Load Type	Rating (W)	Quantity	Consumption time (Hrs/d)	Total consumption (Wh/day)
Lights	15	6	10	900
Roof fan	50	3	16	2400
Air Cooler	75	1	2	150
Television	150	1	2	300
Refrigerator	150	1	16	2400
Mobile Charger	5	2	4	40
Water Pump	500	1	2	1000
The total load for one house				7190
The total load for three houses				21,570

C. HRES STRUCTURE AND COMPONENTS SPECIFICATIONS

Fig. 10 shows the suggested strategy for the optimization of components size with power management for an off-grid HRES. The initial step involves the assessment of real-time meteorological information and the load profile of the suggested site. After specifying the optimization objectives along with constraints, feasible configurations of the HRES, the elaborated model of multiple model components is accomplished. The most feasible model is proposed based on the detailed analysis with the assessment of three aspects i.e. technical, economic and environmental. The next step involves the execution of the suggested EMS for the winning configuration plan. The final step analyzes the validation of the proposed management strategy and its comparison with the conventional method. The description of the proposed HRES, as well as the detailed modeling of system components, are discussed as follows:

The suggested system comprises DG, WT, PV, battery storage, and power converter. PV, Wind, and diesel are considered as the main generation to fulfill the energy requirements. The battery storage is considered to feed load under fluctuating PV and wind generation during different conditions (i.e. transients, ripples, and spikes). The power converters are an essential part of the HRES to supply energy from dc and ac bus. It is significant to mention that the boost converters are used for extracting maximum power from PV and wind, while battery converter (buck-boost) stabilizes the constant dc bus voltage.

1) WIND ENERGY CONVERSION SYSTEM (WECS)

The WECS contains wind turbines, PMSG, and the mechanism for maximum wind power extraction. Wind model from [42] of 1 kW rating is selected, while initial and replacement costs are set to $ 900/kW [61], O&M cost as $ 10/kW with 20 years project life. Wind mechanical power P_{mec} is expressed as:

$$P_{mec} = \frac{1}{2} C_p(\lambda, \beta) \rho \pi R^2 v_w^3 \tag{1}$$

$$C_p = 0.22 \left(\frac{116}{\lambda_i} - 0.4\beta - 5 \right) e^{-12.5/\lambda} \tag{2}$$

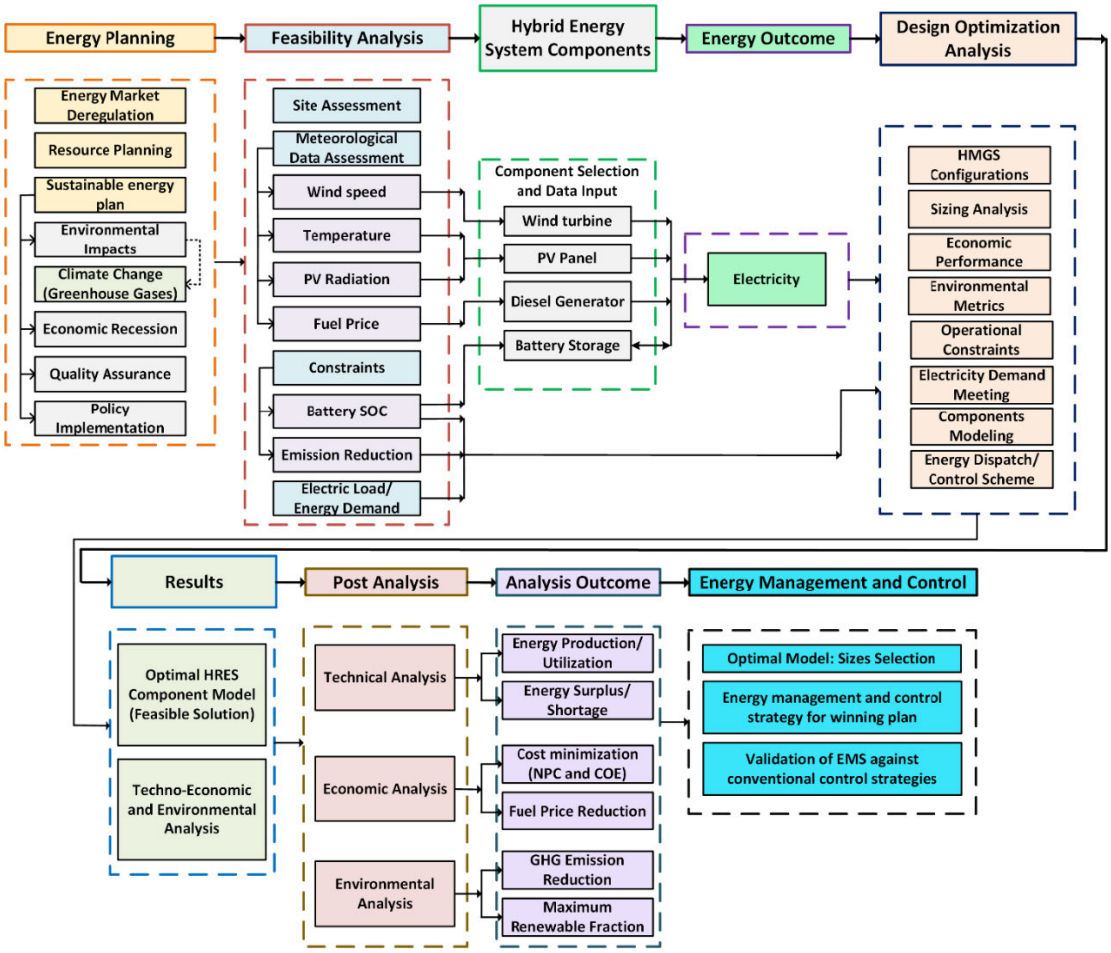

FIGURE 10. The proposed framework for the design optimization, management, and control of standalone HRES.

$$\lambda_i = \frac{1}{\frac{1}{(\lambda+0.08\beta)} - \frac{0.035}{(\beta^3+1)}} \tag{3}$$

The blade tip speed ratio is expressed as

$$\lambda = \frac{\omega_t . R}{v_w} = \frac{k_g . \omega_D . R}{v_w} \tag{4}$$

Fig. 11 shows the maximum values of the power coefficient (Cp) against the tip speed (λ). Normally, the value of the pitch angle is zero when P_{mec} is below nominal power. Hence, Cp is the function of λ only and is maximum C_{pmax} at a specified value of λ as shown in Figure. Blueline with zero angles (beta) shows that the tip speed of 8 units has a maximum power coefficient of 0.48 which is the case of the current wind model in this paper. At this moment, the WT operates at MPPT and the optimal rotor speed ω_{Dopt} specific wind speed of v_w in (4). By substitution of (4) in (1), we get:

$$P^{WG}_{MPPT} = \frac{\rho\pi R^5 k_g^3 C_{p\max}}{2\lambda^3} . \omega_D^3 = C_M . \omega_D^3 \tag{5}$$

The wind MPPT algorithm and the pitch angle control are implemented for maintaining active power (P). The reference P is obtained through the MPPT model based on the present

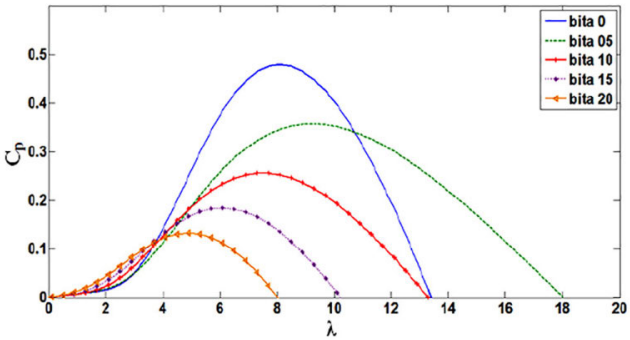

FIGURE 11. Analytical approximation of Cp (k, b) characteristics [38].

rotor speed (ω_D). The relation for automatically reaching optimal rotor speed is expressed as follows:

$$2H_D . \omega_D . \frac{d\omega_D}{dt} = P_{mec} - P^{WG}_{MPPT} \tag{6}$$

Keeping in view the fast-electronic operation, the wind power (P) is assumed to be equal to the reference power.

2) PV GENERATOR

The solar power is comparatively cheap as compared to wind power because of no wear and tear [6]. Incremental

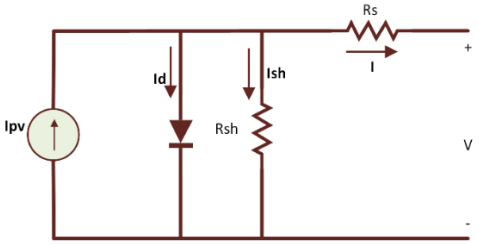

FIGURE 12. Equivalent circuit of single PV cell.

conductance (IC) is a commonly used method for solar PV MPPT which improves steady-state as well as dynamic response with good performance under fast-changing atmospheric conditions. Its basic principle for three MPP tracking conditions states that the power derivative is zero at MPP while it is negative on the right side of MPP and positive on the left side for power versus voltage curve. It can be expressed as [65].

$$\frac{dP}{dV} = \frac{d\,(IV)}{dV} \approx I + V\frac{\Delta I}{\Delta V} \tag{7}$$

The three MPP tracking conditions are represented by Eqs. (8)-(10). $\Delta I/\Delta V$ is incremental conductance, while I/V represents instantaneous conductance.

$$\frac{\Delta I}{\Delta V} = -\frac{I}{V}; \tag{8}$$

$$\frac{\Delta I}{\Delta V} > -\frac{I}{V}; \tag{9}$$

$$\frac{\Delta I}{\Delta V} < -\frac{I}{V}; \tag{10}$$

The clearness index (K_t) is given by [66]

$$K_t = \frac{H_{ave}}{H_{o,ave}} \tag{11}$$

$$H_{o,ave} = \frac{\sum_{n=1}^{N} \frac{24}{n} G_{on}\left(\cos\varphi\cos\delta\sin\omega_s + \frac{n\omega_s}{180^0}\sin\varphi\sin\delta\right)}{N} \tag{12}$$

where H_{ave} and $H_{o,ave}$ are solar radiations and top-of-atmosphere radiations with the following expression. While φ and N are longitudes of the specified location and number of days respectively.

The total PV output current (I) can be calculated as [2]

$$I = N_P I_{PV} - N_P I_O\left\{\exp\left(\frac{V + IR_S}{nV_t}\right) - 1\right\} - \frac{V \times \frac{N_P}{N_S} \times IR_S}{R_{Sh}} \tag{13}$$

where N_P and N_S are respectively the number of cells of PV panel array which are connected in parallel and series. I_{PV}, and I_O are photocurrent of PV cell and reverse saturation current respectively. V, and V_t represent cell rated and thermal voltage while n is diode ideality factor. The intrinsic series and shunt resistances are denoted by R_S and R_{Sh} respectively.

The constraint for solar power generation is [6]

$$0 \le P_{PV}(k) \le P_{PV\,\max}(k) \tag{14}$$

The boost converter is implemented to control the performance of PV panels. the photovoltaic current (I_{PV}) is directly related to insolation (λ_S) as [67]

$$I_{PV} = \left\{I_{SC} + k_{temp} * (T - T_{nom})\right\} * \frac{\lambda_S}{\lambda_{nom}} \tag{15}$$

where I_{SC}, k_{temp}, T_{nom}, and λ_{nom} are short circuit current (SCC), temperature coefficient related to SCC, nominal insolation and temperature respectively.

3) BATTERY ENERGY STORAGE SYSTEM (BESS)

During the intermittent renewables, the HRES reliability can be ensured by using battery storage backup. SPRE 06 415 models of the battery are used with 2.45 kWh nominal capacity, 80 % roundtrip efficiency, and 1958 kWh lifetime (throughput). The initial, replacement, and operating cost is supposed to be $ 176 /unit, $ 176/unit, and $ 8/yr respectively [68]. The minimum and maximum *SOC* range is 20 % and 70 % respectively with 20 % depth of discharge (*DoD*) and fast charging. The calculation for battery size is expressed in Eq. (16) [69].

$$C_{Bat} = \frac{V \times N_{day}}{\eta_{conv} \times \eta_{bat} \times DOD} \tag{16}$$

where V, N_{day}, η_{conv}, η_{bat}, and DOD are no-load voltage, the number of days without charging, converter efficiency, battery efficiency, and depth of discharge respectively.

The mathematical relation for terminal voltage and *SOC* of the battery is expressed in Eqs. (17)- (18) [70].

$$V_{Bat} = V_{out} - i_{bat}R_{bat} - K\frac{Q}{Q - \int i_{bat}dt} + Ae^{(-B\int i_b dt)} \tag{17}$$

$$SOC = 100\left(1 - \frac{\int i_{bat}dt}{Q}\right) \tag{18}$$

Constraints for battery *SOC* are represented in Eqs. (19)-(20) [70].

$$20 \le SOC \le 80 \tag{19}$$

$$-\frac{P_{Bat}}{V_{Bat}} \le I_{Bat} \le \frac{P_{Bat}}{V_{Bat}} \tag{20}$$

The formula for the inductor design of a battery storage unit is defined in Eq. (22) [71].

$$L_{Bat} = \frac{V_{DC}(1 - D)}{2.f_{\min}.\Delta I_B} \tag{21}$$

The parameters for the design of battery inductor include [33] ΔI_{bat} which is 20 % of I_{bat}, while $I_{bat} < I_{bat(max)}$, and $D_{Bat} = V_{DC}/V_{Bat}$.

4) POWER CONVERTER

A dc-ac converter is used to transfer power from dc bus to ac bus with initial and replacement cost of $ 200/kW each, while O&M cost is negligible and set to zero with a lifespan of 15 years and 95 % efficiency.

The relation for the power capacity (C) of the converters is shown in Eq. (22) as [2]

$$C = (3 \times L_{ind}) + L_{res} \tag{22}$$

where L_{ind} and L_{res} are inductive (refrigerator, fan, pump) and resistive (LED lights, TV, mobile charger) loads respectively.

5) DIESEL GENERATOR

A DG is employed to fulfill a high-power deficit during fluctuating generation. The capital and O&M costs are considered as $ 1000/kW and $ 0.05/kW [72], with $ 0.8 fuel price per liter of diesel-based on market trends in Pakistan. A lifetime of 10000 hours and a 25 % minimum DG load ratio is considered. Depending upon output power, the fuel consumption of DG can be estimated from Eq. (23) [72]:

$$F_{DG} = (\alpha \times C_{dg}) + (\beta \times P_{dg}) \tag{23}$$

where F_{DG},α,β,C_{dg},$and P_{dg}$ are fuel consumption rate in Ltr/hr, fuel intercept coefficient in Ltr/kWh, fuel slope in Ltr/kWh, diesel generator capacity in kW, and diesel generator output in kW respectively.

IV. OPTIMAL SIZING AND ECONOMIC ANALYSIS USING HOMER PRO

Different optimization tools compared in [73], are discussed and used in literature to design an optimally planned HRES. Out of 41 software tools mentioned in [74] viz. HYBRID 2 [75], RETScreen [76], iHOGA [77], TRNSYS [78], and IPSYS; and 6 user-friendly tools [79]; HOMER (Hybrid Optimization of Multiple Electric Renewables) software is the most frequently used and highly recommended in various research studies.

HOMER is a robust techno-economic optimization tool [45] which allows adaptability to analyze and simulate techno-economic models and design optimization of HRES units [45].

Its optimization algorithms allow the designer as well as the decision-makers to estimate the feasibility in terms of economic and technical aspects with various technical selections regarding the fluctuations in technology costs as well as the availability of resources. Hence, HOMER is selected for techno-economic analysis to determine the most suitable model choice for fulfilling the load demand of the suggested location.

HOMER evaluates quickly and easily for feasible and optimal plans out of various possible solutions. The proposed optimization flow chart is shown in Fig. 13. HOMER optimizes the sizes of PV panels, the number of wind turbine units, the number of battery storage units, and the a number of converters [2]. HOMER optimization is based on the input parameters including load demand, energy resources data, economic and technical aspects of each component, design constraints, proposed management, and control strategy, emission data [2], [45] with total NPC as the objective function of optimization strategy [45]. HOMER analysis is based on one-year optimization for the evaluation of technical, environmental, and economic aspects of HRES [80].

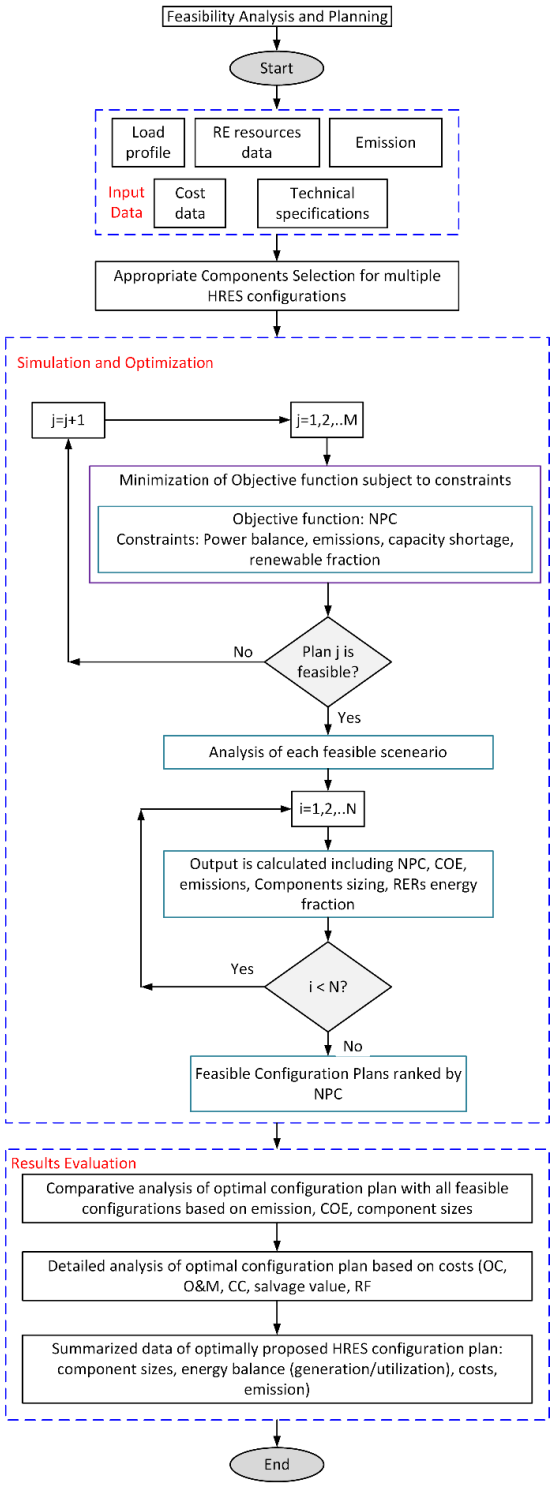

FIGURE 13. Implemented methodology for HRES design optimization.

Afterward, extrapolation of all costs works for the rest of the years throughout the project lifetime, which is established on linear depreciation and the most feasible plans to guarantee uninterruptible power supply and energy demand balance based on hourly duration [45]. After completing the testing step for all potential plans of HRES, the feasible configurations are found and graded on the basis of design objectives.

The past studies presented different evaluation criteria mentioned in [42] are used to find the feasible plan of HRES. In this work, TNPC and LCOE are used as the main objective function of the proposed HRES with mathematical relations are expressed as

$$NPC = \frac{C_{t,ann}}{CRF} \tag{24}$$

$$CRF = \frac{j(j+1)^n}{j(j+1)^n + 1} \tag{25}$$

$$COE = \frac{C_{ann,t}}{E_{ann,t}} \tag{26}$$

$$j = \frac{j-k}{1+1} \tag{27}$$

where, $C_{ann,t}$ shows the total HRES annual cost in \$/yr while CRF represents capital recovery factor, j, *and* k are the annual interest and inflation rate in % and n is project lifetime in years, respectively and $E_{ann,t}$ is maximum load supplied in kWh/yr. The expression for renewables shares [107] is written as

$$RF = 1 - \frac{E_{NR}}{E_S} \tag{28}$$

where E_{NR} and E_S are the non-renewable energy and total energy supplied to the load respectively. The power balance constraint is expressed in Eq. (29) which shows that the sum of consumed power is equal or less than the generated value [81].

$$\sum_{j=1}^{N} P_{PV} + \sum_{j=1}^{N} P_{WT} + Pdiesel + P_{bat} - P_{load} = 0 \tag{29}$$

where P_{PV} and P_{WT} are the output power of i^{th} PV and WT unit respectively. Further, the power limits of energy generation and battery operating limits [81] is satisfied i.e.

$$P_{ch\arg e}^{\max} \le P_{bat} \le P_{disch\arg e}^{\max} \tag{30}$$

where P_{charge}^{max} and $P_{discharge}^{max}$ shows the maximum charge and discharge power of the battery.

The diesel generator produces harmful emissions out of which carbon dioxide is the main emission which is considered in the proposed system with the following relation in Eqs. (31)-(33) [82].

$$CO_{2W} = \frac{C_C.E_{DG}}{1016.04} \tag{31}$$

$$CO_2 = \left(\frac{E_{TRC}}{C_C}\right).1016.04 \tag{32}$$

$$P_C = CO_{2W}.CO \tag{33}$$

V. TECHNICAL ANALYSIS USING MATLAB

A. FCS-MPC FOR RECONFIGURABLE INVERTER

Finite control set MPC is suggested for dc-ac interlinking converter control for regulation of load voltage magnitude. FCS-MPC for two-level three-leg voltage source inverters is analyzed in this paper. The presented control scheme selects the most optimal state out of all seven possible switching states to minimize the cost function. Simulation studies of MPC based control scheme show compensation of perturbation in load, source and filter parameters with output voltage is continuously tracking the reference value without sacrificing normal inverter operation. A dc-dc battery converter is applied to regulate the dc voltage. PV and wind converters are applied for extracting maximum power from PV and wind units. Step by step control and management strategies are discussed in detail in the following section.

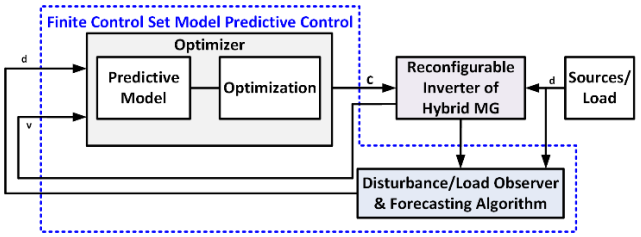

FIGURE 14. Applied FCS-MPC control for a reconfigurable inverter of HMG.

Fig. 14 shows the concept of the MPC control strategy. the variables which are needed to handle and solve the specific problem are represented by v. The disturbance is represented with d. the control variable is expressed by c. w is the forecasted value of the processed variable. Based on the measurements of the present system (v) and disturbances/forecasted values (d), the optimizer can be simulated.

FCS-MPC scheme is applied for primary control of the interlining voltage source inverter, including power droop control, reference generator (three-phase), and inner control loop. In contrast to conventional controllers, FCS-MPC has no requirement of PI controllers to implement the inner current and outer voltage control loop or any other complex modulation steps (like PWM and SVPWM) while this online optimization scheme is quite simple and intuitive with the fast-dynamic response as compared to the traditional control schemes. The working principle of the FCS-MPVC control mechanism is discussed in the sections below.

In the first step, Clark transformation is applied to convert voltage signals from abc to α-β reference, which are the inputs for the inner loop. Measurement of RLC filter is used to generate the switching signals for interlining VSI. The measurements of RLC filters which are taken from primary control are then used to calculate instantaneous powers (P and Q) while fundamental powers are also calculated. Droop control strategy with $P-V$ and $Q-\omega$ is implemented for regulating the ac bus voltage. The final reference signals for VSI transistors (MOSFETs) are generated by using a three-phase sinusoidal generator to regulate the voltage. Discrete-time state-space modeling is implemented with the help of RLC parameters. FCS-MPVC based algorithm is used to predict voltage values for all fourteen (14) combinations for the next sampling duration.

The continuous state-space (CSS) model is designed in the discrete-time state-space (DSS) model. MPC algorithm predicts voltage vectors for all possible combinations for the

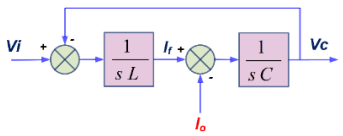

FIGURE 15. Filter model for Predictive voltage control.

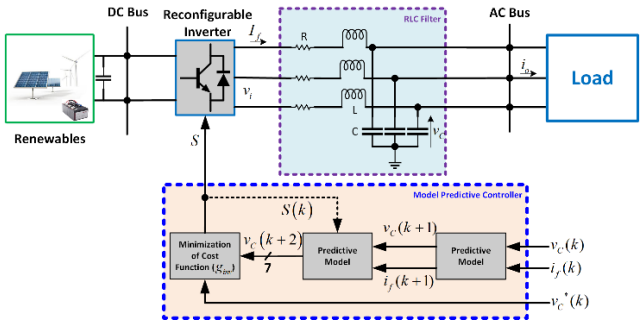

FIGURE 16. FCS-MPC scheme for interlinking converter.

next sampling time. CSS and DSS models, input voltage vector, and objective functions are expressed in [42]. Seven switching states are tested to find the most optimal voltage vector and its corresponding signals for the IGBT switches of VSI.

The filter model (see Fig. 15) for Predictive voltage control of Fig.16 is

$$\frac{d}{dt}\begin{bmatrix} i_f \\ v_c \\ i_o \end{bmatrix} = \begin{bmatrix} 0 & -\frac{1}{L} & 0 \\ \frac{1}{C} & 0 & -\frac{1}{C} \\ 0 & 0 & 0 \end{bmatrix} \begin{bmatrix} i_f \\ v_c \\ i_o \end{bmatrix} + \begin{bmatrix} \frac{1}{L} \\ 0 \\ 0 \end{bmatrix} v_i + \begin{bmatrix} 0 \\ 0 \\ f(i_o, v_c) \end{bmatrix} \quad (34)$$

where V_c, V_i,I_f, R_f, and L are load side voltage vector, inverter output voltage, filter current, and filter resistance, and inductance. CSS model can be expressed as

$$\frac{dx}{dt} = Ax + Bv_i + u_d(k) \quad (35)$$

To predict the voltage, DSS modeling is obtained as

$$x(k+1) = A_q x(k) + B_q v_i(k) + u_d(k) \quad (36)$$

By for the DSS model, we obtain

$$\begin{bmatrix} V_c \\ I_f \end{bmatrix}^{k+1} = A_d \begin{bmatrix} V_c \\ I_j \end{bmatrix}^{k} + B_d \begin{bmatrix} V_i \\ I_o \end{bmatrix} \quad (37)$$

$$Where\ A_q = e^{AT_s},\ B_q = \int_0^{T_s} e^{A\tau} Bd\tau$$

and V_i is input voltage vector with seven possible switching states for inverter (VSI) switches (S_a, S_b, S_c) as:

$$V_n = \begin{cases} \frac{2}{3} V_{dc} e^{j(n-1)\frac{\pi}{3}} & for\ n = 1, 2, \ldots 6 \\ 0 & for\ n = 0, 7 \end{cases} \quad (38)$$

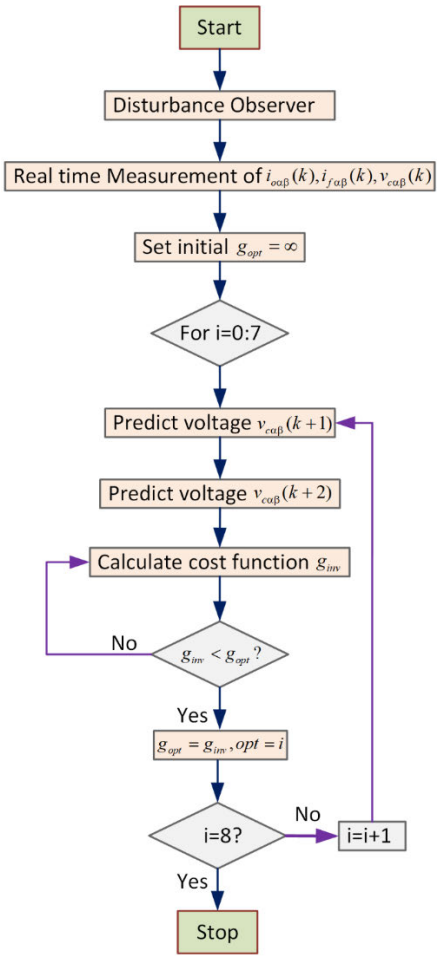

FIGURE 17. The flow chart of the implemented FCS-MPC algorithm.

The load observer is suggested with the following cost function,

$$g_{inv} = (v^*_{c\alpha} - v_{c\alpha})^2 + (v^*_{c\beta} - v_{c\beta})^2 \quad (39)$$

Fig. 17 shows the flow chart of the applied algorithm for inverter control in islanded mode.

The active power is regulated through the voltage magnitude of the inverter output, and the reactive power is controlled through the inverter frequency. Voltage amplitude (V_{nom}) and angular frequency (ω_{nom}) of the inverter output voltage is utilized to control power flow (active and reactive) through distributed energy resources (DERs) in an ac microgrid as described in expressions (40) and (41).

$$\omega_i = \omega_{nom} - m_i P_i \quad (40)$$

$$V_i = V_{nom} - n_i Q_i \quad (41)$$

The coefficients (m and n) are selected based on the following relations to ensure system stability.

$$m_i = \frac{\Delta\omega}{Q_{\max}} \quad (42)$$

$$n_i = \frac{\Delta V}{P_{\max}} \quad (43)$$

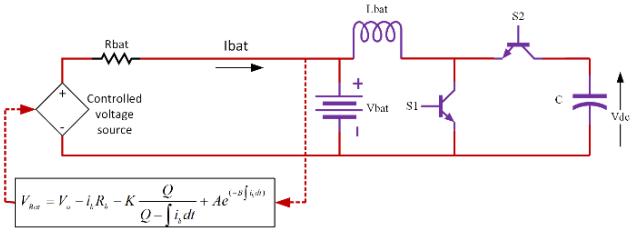

FIGURE 18. Battery model.

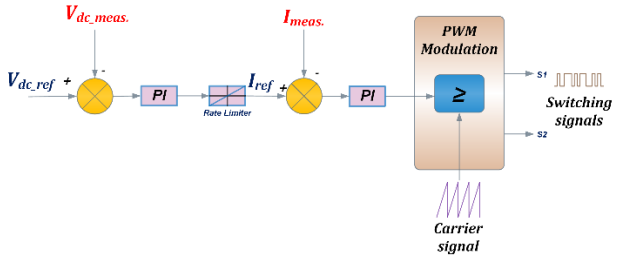

FIGURE 19. A buck-boost converter control.

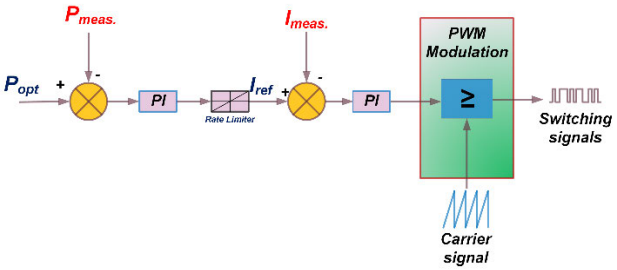

FIGURE 20. The boost converter control for wind MPPT.

where $P_{\max}$ and $Q_{\max}$ are the maximum powers supplied by the inverter. $\Delta\omega$ and ΔV are maximum deviations of frequency and voltage amplitude of the inverter output. The values of m and n are 0.0014 and 0.0008 respectively.

B. BUCK-BOOST BATTERY CONTROLLER

For the regulation of dc bus voltage, Fig. 18 shows the battery model while Fig. 19 shows the control of a buck-boost converter, which comprises current and voltage regulators.

The *SOC* is controlled from being discharged below 20 % and overcharged above 70 %. The net power is the summation of generated power from PV, WT, and DG, plus the load power which can be expressed by Eq. (44).

$$P_{net} = P_{PV} + P_{Wind} + P_{Diesel} + P_{Load} \tag{44}$$

The battery SOC management scheme along with the applied dispatch strategy is demonstrated in Fig 22. Fig 26 presents the complete Simulink model of the most optimal HRES with PV-wind-battery units.

C. BOOST CONVERTER CONTROL

Wind generator with a fixed pitch angle (i.e. zero) and variable speed is used, while the PMSG parameters and WT parameters are taken from [42]. Fig.20 shows the MPPT control for the boost converter.

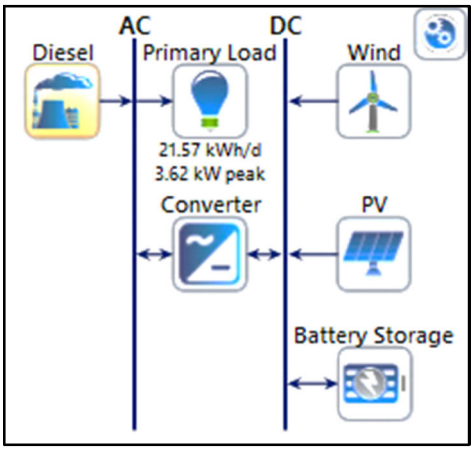

FIGURE 21. HOMER model for the proposed HRES.

VI. RESULTS AND DISCUSSIONS

A. OPTIMAL DESIGN AND PERFORMANCE ANALYSIS USING HOMER PRO

The economic aspects and technical data for every HRES component including PV, WT, DG, BSS and converter based on the load profile data, real-time PV irradiance/temperature and wind speed are investigated. The following assumptions and constraints are considered for modeling and simulation of HRES shown in Fig. 21.

- Project lifetime is considered to be twenty years in order to obtain level best computation of the HRES.
- The nominal discount rating is considered to be 10 % based on trends in Pakistan with 4 % inflation.
- The maximum reliability is ensured by considering zero capacity shortage during the simulation of the system.
- A 10 % reserve is considered to compensate for the abrupt load variations and spikes. The wind energy reserve is chosen to be 15 % for compensating random speed variations.
- A carbon penalty cost of $ 20/tons is taken as a constraint.
- Energy flow between different components is controlled by applying the suggested dispatch methodology. Fig 22 shows the flow chart to generate enough power from diesel which can fulfill load demand. Battery charging and serving deferrable load is set as low priority objectives which are dependable on renewable energy generation. LF methodology is suitable for achieving maximum benefits from renewables and reducing fuel consumption i.e. reducing working hours of diesel generator. LF also saves the battery from over charging-discharging [40]. Optimized results of all feasible configuration plans of the suggested HRES based on techno-economic analysis are shown in Table 7. which are ranked based on NPC. The following are the concluding remarks about these results.
- Out of all possible configuration plans, PV-wind-battery-converter has superior performance as well as

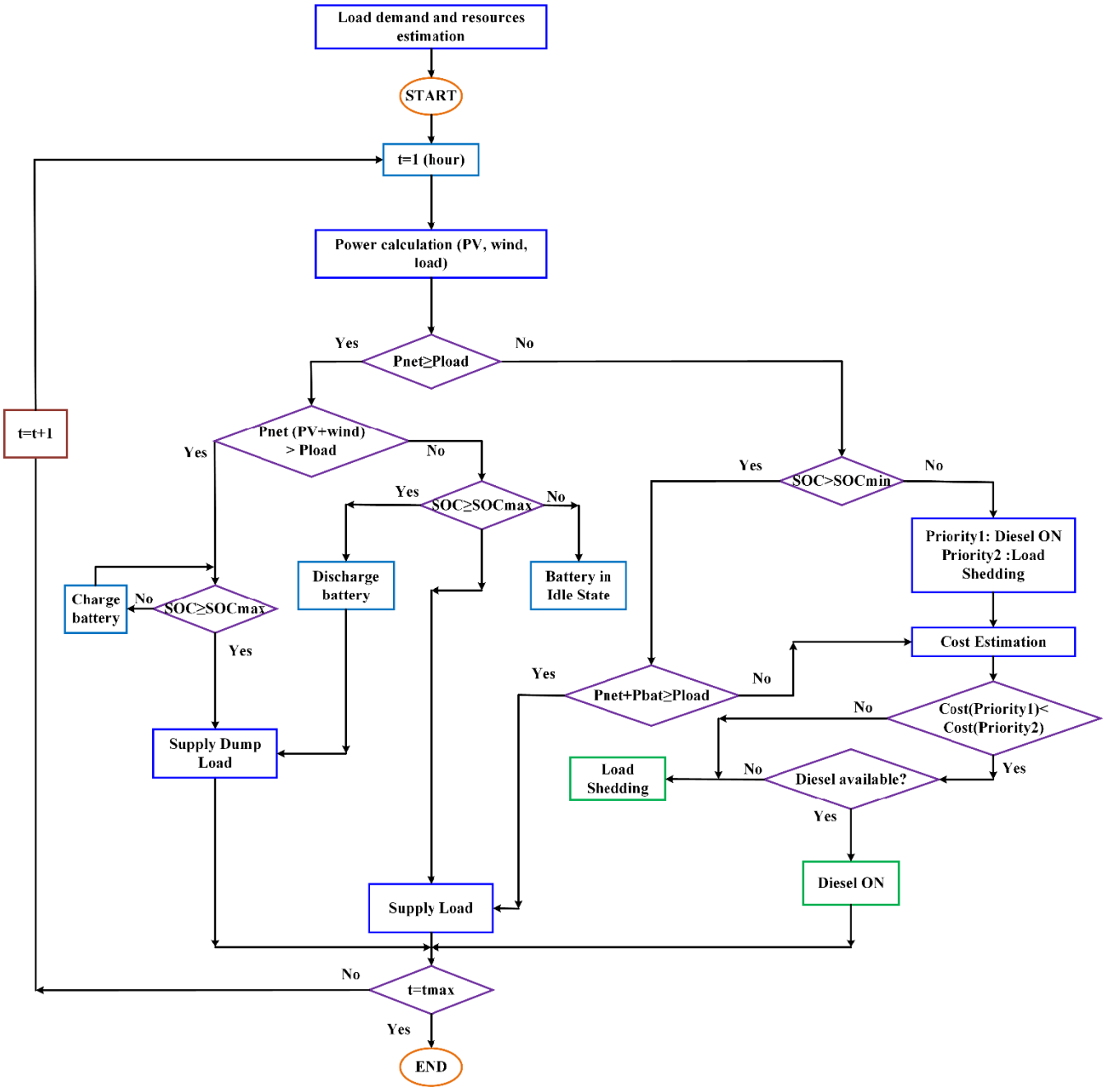

FIGURE 22. Applied dispatch method for PV/diesel/battery HES.

the most feasible plan of the suggested HRES to supply the highlighted remote area with excess electricity of 2030 kWh per year (i.e. 30.1 %).

- The winning configuration plan as shown in Table 6 comprises 13.4 kW PV, four (4) wind turbines (1 kW each), twenty (20) batteries (2.37 kWh), and 3.88 kW converter.
- The obtained optimal HRES plan attained the least possible NPC ($ 28,620), COE ($ 0.311/kWh), 100 % renewable penetration (RF) without any fuel consumption as well as emission. These results will definitely serve as a viable option for remote area HRES in Pakistan based on techno-economic and environmental criteria.
- The base scheme (i.e. diesel only) is the normal trend in Pakistan which is proved to be the worst-case scenario in this study with the highest NPC ($ 156,037), COE ($ 1.700/kWh). O&M cost ($ 12,666), annual fuel consumption (4,571 L/yr) and carbon emission penalty (11,965 kg/yr).

Fig. 23 shows the generated electricity sharing on a monthly basis between PV and wind. Maximum PV and wind

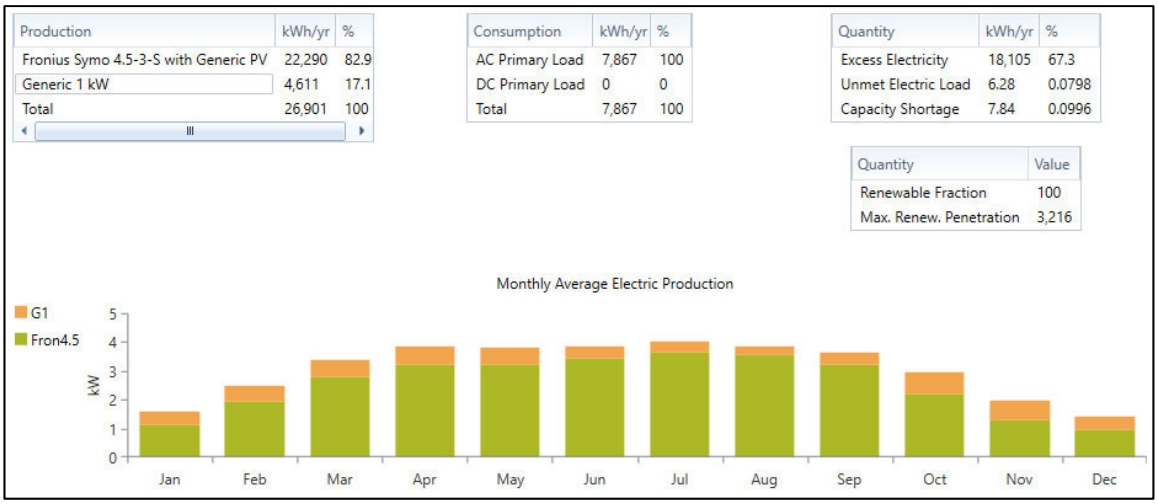

FIGURE 23. Power generation on a monthly basis along with energy generation and utilization.

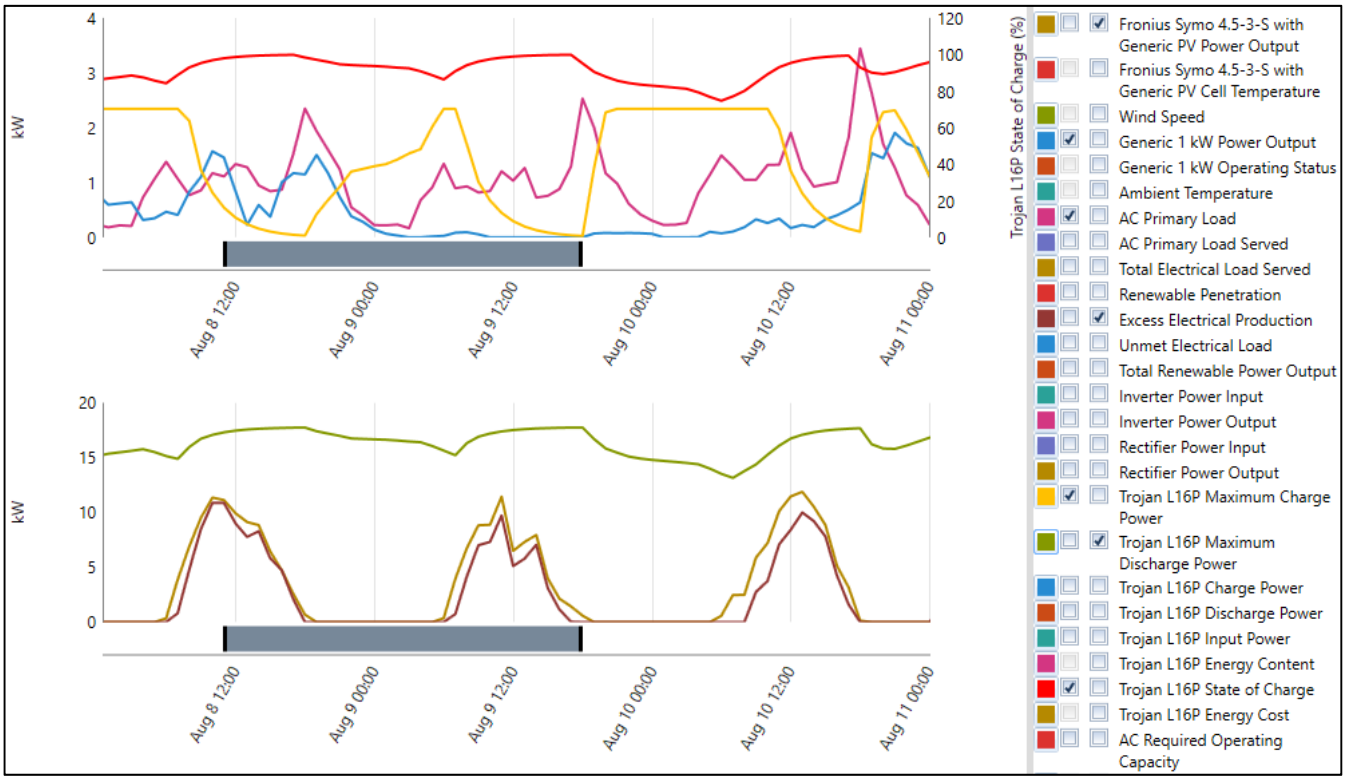

FIGURE 24. Energy scheduling for the optimal configuration of HRES system (sample days: August 8-11).

TABLE 6. Results of the optimal HRES.

Cost ($) / Comp.	*Capital*	*O&M*	*Replacement*	*Salvage*	*Total*
Battery Storage	3,500	1,870.07	0.00	187.65	11,520.53
Power Converter	1,163.75	0.00	501.73	252.69	1,412.80
PV	10,748.61	1,570.36	0.00	700.16	11,618.82
WT	3,600.00	467.52	0.00	0.00	4,067.52
System	19,012.37	3,907.95	6,652.20	952.84	28,619.67

generation is extracted to achieve the required load demand. It is observed from Fig. 23 that the PV generation is maximum in July due to highest daily radiations i.e. 6.892 kWh/m^2 followed by the month of June which has second-highest radiations i.e. 6.877 kWh/m^2 and it can also be verified from Fig. 7.

The real-time energy scheduling of generation and utilization is shown in Fig. 24 for the selected (sample) days i.e. from August 8 to August 11.

A deep investigation of Fig. 24 discloses important aspects of the proposed HRES with a winning configuration plan. It is depicted that the PV generation is slightly higher than the excess electricity generation. It shows that most of the PV generation is in excess and it can be managed for other

TABLE 7. All feasible plans with technoeconomic based optimization.

Sc.	HRES configuration	Component size					Economic indicators				RF (%)	Fuel (L/yr)
		PV (kW)	WT (units)	DG (kW)	Converter (kW)	BESS (units)	Initial ($)	O&M ($/yr)	NPC ($)	COE ($/kWh)		
1	PV-WT- Battery-Converter	13.4	4	-	3.88	20	19,012	821.98	28,620	0.311	100	0
2	PV-WT-DG-Battery-Converter	7.39	3	4.00	3.65	12	19,811	805.76	29,229	0.318	93.5	239
3	PV-Battery-Converter	16.9	-	-	4.81	28	19,844	1,081	32,474	0.353	100	0
4	PV-DG-Battery-Converter	12.3	-	4.00	3.66	18	22,103	980.72	33,565	0.365	94.0	223
5	WT-DG-Battery-Converter	-	15	4.00	3.30	32	28,091	2,316	55,166	0.599	85.9	509
6	PV-WT-DG-Converter	8.69	15	4.00	3.32	-	29,449	5,018	88,095	0.957	49.5	1,813
7	PV-DG-Converter	11.0	-	4.00	2.06	-	17,419	7,840	109,055	1.190	17.6	2,894
8	WT-DG-Converter	-	25	4.00	3.31	-	31,494	7,136	114,903	1.250	31.1	2,502
9	DG-Battery-Converter	-	-	4.00	0.969	6	9,341	10,367	130,509	1.420	0.00	3,683
10	DG (base case)		-	4.00	-	-	8,000	12,666	156,037	1.70	0.00	4,571

applications like solar water heating and home cooling system. The second alternative way to use this PV excess energy is to widen the feeding remote area by including more houses which is one of the important points to keep for future research. The battery *SOC* remained within permissible limits above 20 % to avoid over-discharging of the battery storage units, while the maximum battery discharge power is linearly dependent on *SOC* pattern. The maximum load demand is observed at about 6 am (August 8) in the morning when maximum utilization of electricity is obvious due to wake-up time for cooking breakfast and preparing for children for schools and men/ladies for jobs. At this time, PV and wind are unable to fulfill the required demand and hence the battery is discharged to fulfill the energy shortage gap. At about 11 am on August 8, the PV and wind are sharing maximum energy and all this energy is fully utilized to feed the increasing demand of load with minimum charging power of the battery. The first load peak is observed at about 1800 in the evening when wind generation is maximum while PV generation is almost negligible due to the absence of the sunshine. At this stage, the energy gap is fulfilled by utilizing the battery power while keeping its charging power very low. The same trend of load variations is observed for the rest of the days i.e. August 9-11, with the highest load peaks in the evening at about 1900.

Table 6 summarizes the cost results of the suggested optimal model. The initial cost of PV is three times that of wind. While battery storage units have the almost same cost as that of wind. The O&M cost of the battery is slightly more than PV, while it is four times higher than that of wind. If we compare total cost which includes capital, O&M, replacement, and salvage, then PV and battery storage have almost the same while wind has three times less cost as compared to PV and battery storage.

Fig. 25 shows the nominal cash flow of base case (diesel only) and the most optimal plan (PV-wind-battery) for the duration of 20 years. Minimum cash flow is maintained for the optimal plan throughout the project lifetime, while the cash flow for the base case is continuously increasing until it reaches the maximum value at the end of the entire project life.

B. PERFORMANCE ANALYSIS OF PROPOSED ENERGY MANAGEMENT AND CONTROL SCHEME

An energy management and control schemes are implemented based on the FCS-MPC model keeping in view the fluctuating load demands and intermittent renewable generation as shown in Figure 26. The parameters of PI controllers are shown in Table 8, while Table 9 shows the ratings of PV, wind and RLC filters.

1) MPC CONTROL WITH SOC UPPER LIMIT USING PV-MPPT

Fig. 26 is analyzed to check the operation of the suggested model. Variable wind speed changing from 7.45 m/s (at 5 s) to 6.95 m/s (at 13s) is applied (see Fig. 27), while variable PV irradiance fluctuating from 980 kWh/m^2 (at 5 s) to 1200 kWh/m^2 (at 16 s) is applied. During wind speed variation at 13s, the power coefficient curve shows a slightly spike from its normal value of 0.48 which is negligible. The regulated power coefficient which exactly follows the reference value shows efficient and intelligent design and performance of the MPPT wind controller through a dc-dc converter. The maximum value of 0.48 is achieved at a tip speed ratio with a value of 8 as shown in Fig. 28 (a).

Fig. 28 (b) shows the dc bus voltage which is controlled by applying a dc-dc battery converter to stabilize the voltage at a constant dc voltage of 750 V. Based on the energy

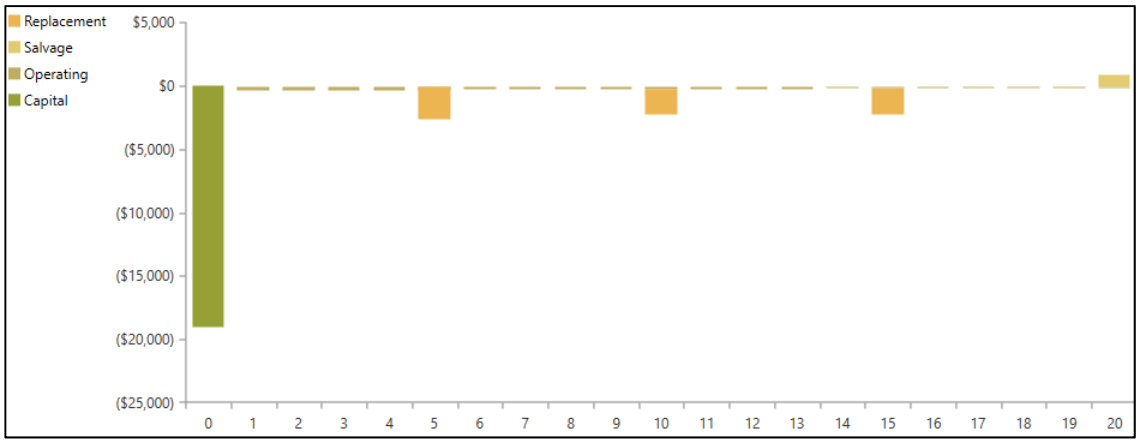

(a) Optimal case

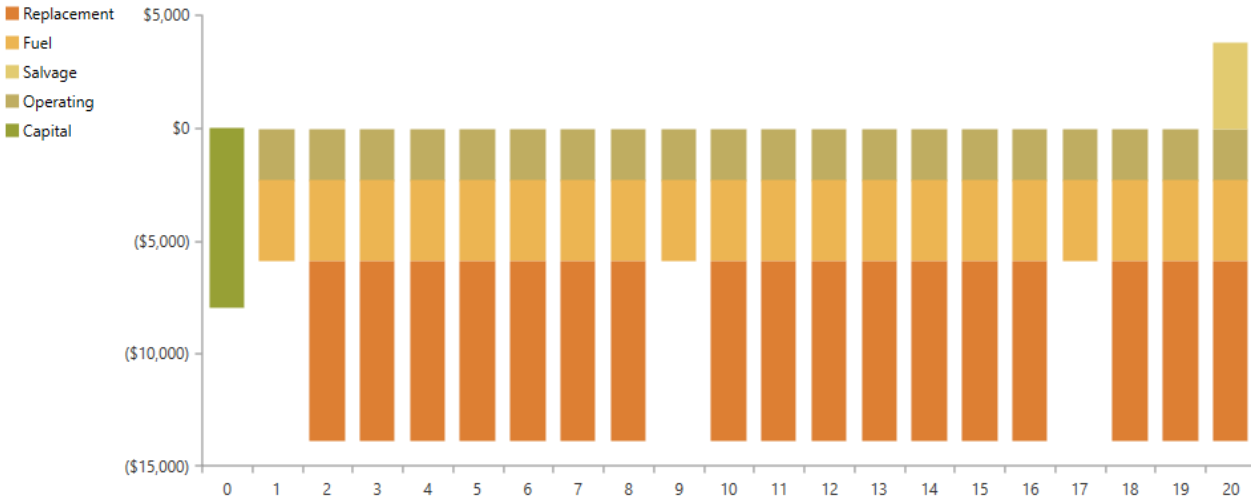

(b) Base case

FIGURE 25. Nominal cash flow results.

TABLE 8. PI controller parameters.

Parameter	*Kp*	*Ki*
Boost controller	0.051	1.000
Battery controller (inner loop)	4.983	10.752
Battery controller (outer loop)	0.449	1.065

TABLE 9. Parameters details of PV, wind and RLC filter.

Parameter	*Value*
PV module type	SunPower SPR-305
Maximum PV power	16.5 kW
Maximum wind Power	4 kW
Filter resistance (R)	0.1 Ω
Filter inductance (L)	7.5 mH
Filter capacitance (C)	250 µF

management and control strategy of Fig. 26, the primary load is continuously ON which can be verified from the load power of Fig. 29, current magnitude and load switch status as shown in Fig. 30. Battery SOC as shown in Fig. 30 remained greater than 20 % (lower limit) while the battery is continuously charging due to excess power generated from PV and wind until SOC reaches 70 % (upper limit) at 8.262 s. At this moment, the secondary load is switched ON which can also be verified from the load power of Fig. 29 (a), and three-phase load current magnitude of Fig 30 (a) while keeping the load voltage constant through FCS-MPVC as shown in Fig. 29 (b).

The performance of the battery controller can be examined from Fig. 28 (b) that the minor voltage reduction at 8.262s is observed during the application of power management strategy with battery SOC. During wind power reduction at 13 s, the battery is absorbing less power to main the load requirement under low wind power while the negligible increase in dc bus voltage due to wind power reduction is observed. At 16 s, PV generation is increased from 13.4 kW to 16.6 kW due to variation in PV irradiance. The increase in dc bus voltage is comparatively higher as compared to the previous two cases when load and wind power variation is observed at 8.262 s and 13 s respectively. FCS-MPVC for

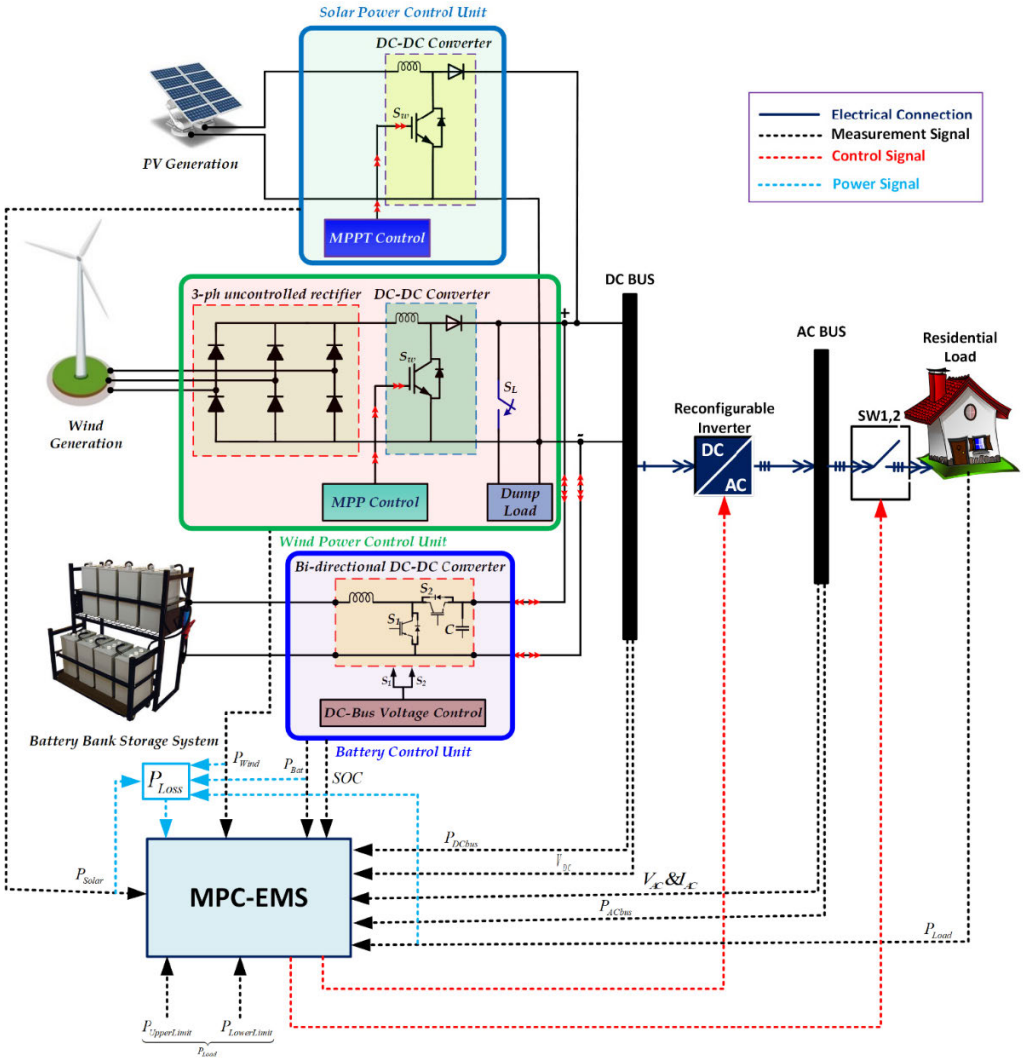

FIGURE 26. The control scheme of an optimal PV-Wind-battery HRES.

interlinking converter effectively regulated the three-phase load voltage during external load disturbance.

2) MPC CONTROL WITH SOC LOWER LIMIT USING PV-MPPT

Fig. 20 is analyzed to check the operation of the suggested model. To elaborate on the operating principle of EMS with a lower *SOC* limit, battery SOC is kept below 20 %.

Critical load i.e. the main load is ON while non-critical loads (i.e. primary and secondary) are both OFF as shown in Figs. 33. Fig. 31 shows the power-sharing among PV, wind, load, and battery and dc bus voltage. During the start of simulation at 5 s when both PV and wind are integrated for power-sharing, ripples in PV power dc bus voltage are observed. The possible reason for these ripples is the minimum load requirement while the MPPT controller performance is not satisfactory which contributes ripples to PV power and ultimately dc bus voltage is also disturbed. The other possible reasons and its remedy may be explored in future research. At 7.595 s, battery SOC reaches a minimum set limit of 20 % and EMS enabled switch-1 to ON position to inject primary load into the system which can be seen from Fig. 31, Fig. 32, and Fig. 33 by observing load power, load current, and load switch-1 respectively.

A dc bus voltage remained constant during this load disturbance. At 13 s, wind power is reduced while battery charging power is also decreased to fulfill this energy gap. Fig. 32 shows the regulated and pure sinusoidal waveform which validates the robust performance of the FCS-MPVC strategy. Secondary load remained OFF throughout the simulation because of the SOC value below its upper limit of 70 %. At 16 s, excess power generated due to the power from PV is absorbed by the battery to maintain the constant load demand and fixed wind power generation. A dc voltage is slightly increased due to high power injection from the PV generator.

3) PI CONTROL WITH SOC UPPER LIMIT USING PV-MPPT

Fig. 20 is analyzed to check the operation of the suggested model with PI control. The PV-wind-battery model is simulated with the implementation of the PV-MPPT algorithm

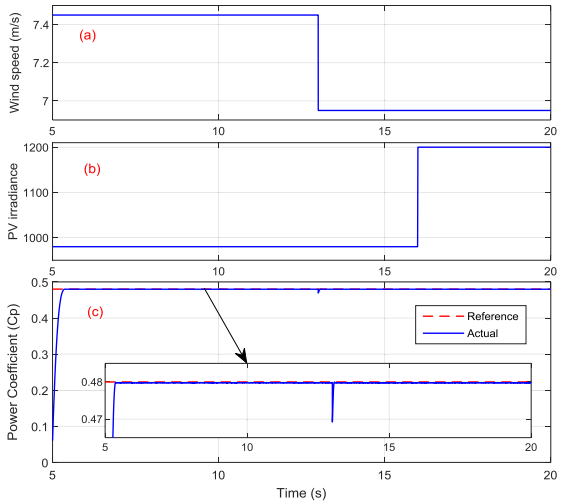

FIGURE 27. Input indicators of PV and WT (a) Variable wind speed (b) Variable PV irradiance (c) Power coefficient.

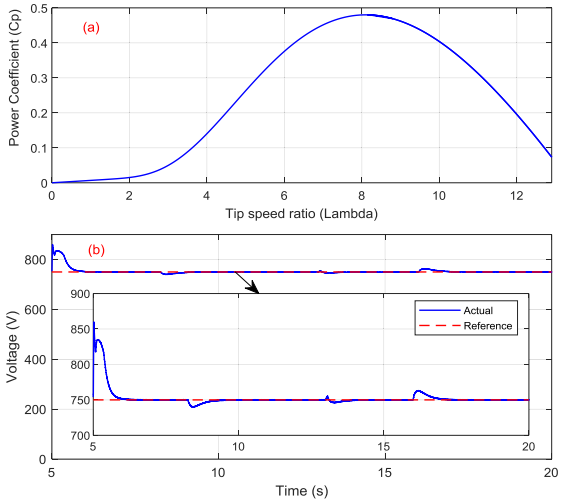

FIGURE 28. WT indicator and dc bus voltage (a) Tip speed ratio against power coefficient (b) A dc voltage regulation by using a buck-boost controller.

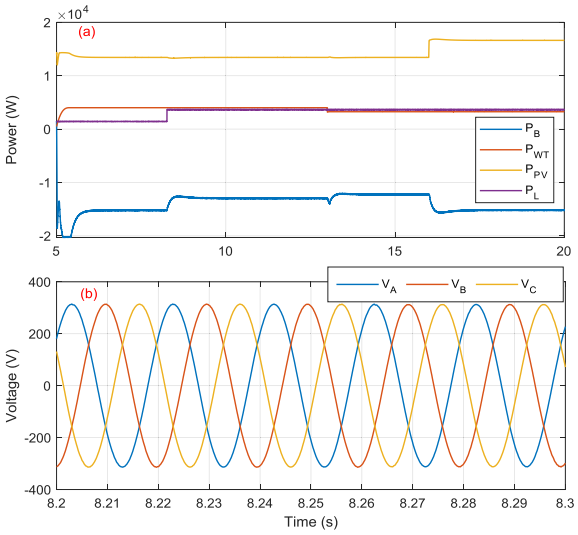

FIGURE 29. Performance analysis of output power and voltage using FCS-MPC method with upper SOC limit and PV MPPT (a) Power-balance among PV, wind, battery, and load (b) Three-phase ac load voltage.

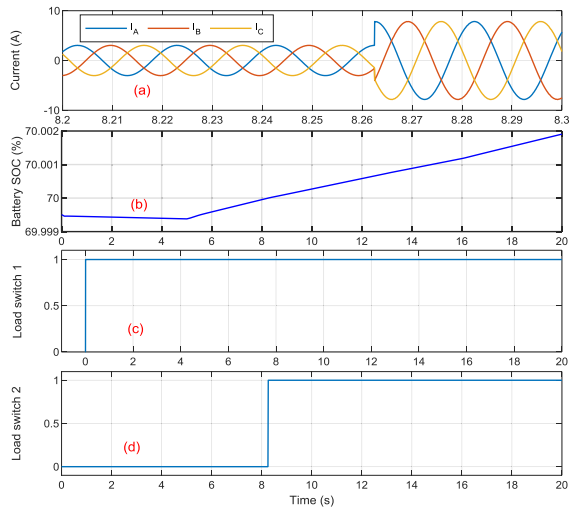

FIGURE 30. Parameters of Load fluctuation with battery SOC using FCS-MPC method with upper SOC limit and PV MPPT (a) Three-phase ac current (b) Battery SOC during charging mode (c) Load switch-1 for primary load control (d) Load switch-2 for secondary load control.

by using the PI control strategy. The model is analyzed for the upper SOC limit of the battery. Fig. 34 shows a three-phase load current and voltage. Power- exchange among PV, wind, battery, and load is shown in Fig. 35. At 8.869 s, battery SOC reaches 70 % (i.e. upper limit) while suggested EMS strategy switched ON the secondary load. The three-phase current and voltage waveforms have different peaks for each phase. Further, more load power ripples are observed in the case of PI control.

4) PI CONTROL WITH SOC LOWER LIMIT USING PV-MPPT

To check the performance of the suggested model with PI control, the PV-wind-battery model is simulated with the implementation of the PV-MPPT algorithm by using the PI control strategy. The model is analyzed for the lower SOC limit of the battery. Fig. 36 shows a three-phase load current and the three-phase ac voltage. Power- exchange among PV, wind, battery, and load is shown in Fig 37. At 8.155 s, battery SOC reaches 20 % (i.e. lower SOC limit) as shown in Fig 37 while suggested EMS strategy switched ON the secondary load. The three-phase current and voltage waveforms have different peaks for each phase. Further, more load power ripples are again observed in the case of PI control.

5) MPC CONTROL WITHOUT PV-MPPT

To check the operation of the suggested model without PV-MPPT, the PV-wind-battery model is simulated without implementing the PV-MPPT algorithm for performance comparison of both models by using FCS-MPVC strategy.

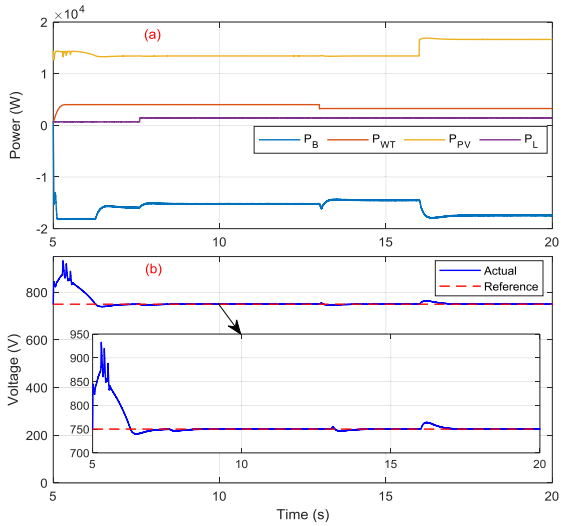

FIGURE 31. Performance analysis of power and dc voltage using FCS-MPC method with lower SOC limit and PV MPPT (a) Power- exchange among PV, wind, battery, and load (b) A dc voltage at variable wind speed.

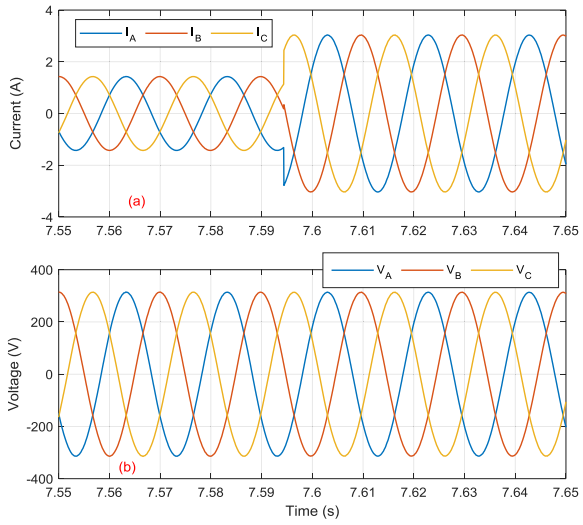

FIGURE 32. Output load signals using FCS-MPC method with lower SOC limit and PV MPPT (a) Three-phase current (b) Three-phase voltage.

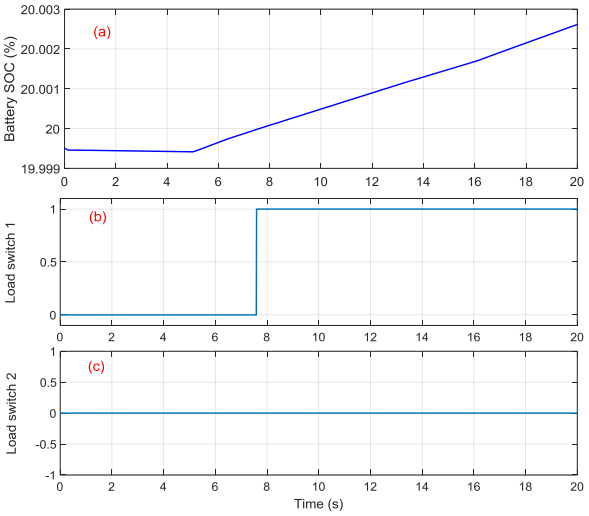

FIGURE 33. Analysis of battery SOC with load management using FCS-MPC method with lower SOC limit and PV MPPT (a) Battery SOC lower limit during charging mode (b) Load switch-1 for primary load control (c) Load switch-2 for secondary load control.

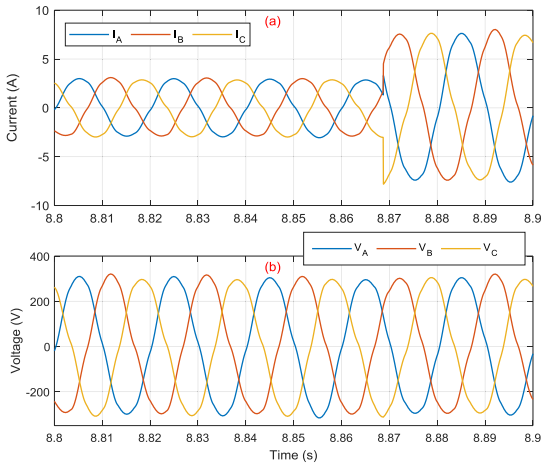

FIGURE 34. Output signals during PI control method with upper SOC limit and PV MPPT (a) Three-phase ac current (b)Three-phase ac voltage.

PV panel is connected with the rest of the HRES through the capacitor link. PV temperature is constant at 25 ° (see Fig. 38) while PV irradiance is changed from 1000 kWh/m^2 (at 5 s) into 950 kWh/m^2 (at 16 s). Wind speed is set at 8.8 m/s at 5 s and decreased to 8.3 m/s at 13 s. A dc voltage is seen to be more stable as shown in Fig. 39 despite the fact that uncontrolled PV generation has variable although stable power. At 9.71 s, battery SOC crosses the upper limit of 70 % (see Fig. 40) and hence the EMS enabled switch-2 to feed the secondary load which can be observed from the load power signal of Fig. 39 and three-phase load current curve of Fig. 40. Fig. 40 (b) shows the regulated ac load voltage under the FCS-MPVC control strategy.

It is observed from Fig. 39 that the variation of wind and load has a direct impact on PV generation fluctuation. This effect of PV fluctuation is observed at 9.71 s when the secondary load is switched ON. The second effect is observed at 13 s when wind generation capacity is reduced by reducing the wind speed, while the last impact is seen at 16 s when PV power itself is decreased by reducing the PV irradiance.

6) PI CONTROL WITHOUT PV-MPPT

To check the performance of the suggested model with PI control, the PV-wind-battery model is simulated without implementing the PV-MPPT algorithm by using the PI control strategy. Fig. 41 shows a three-phase load current and the three-phase ac voltage. Power- exchange among PV, wind, battery, and load is shown in Fig. 42. At 9.866 s, battery *SOC* reaches 70 % (i.e. upper limit) as shown in Fig 42 while EMS activates the secondary load. The three-phase current and voltage waveforms have different peaks for each phase.

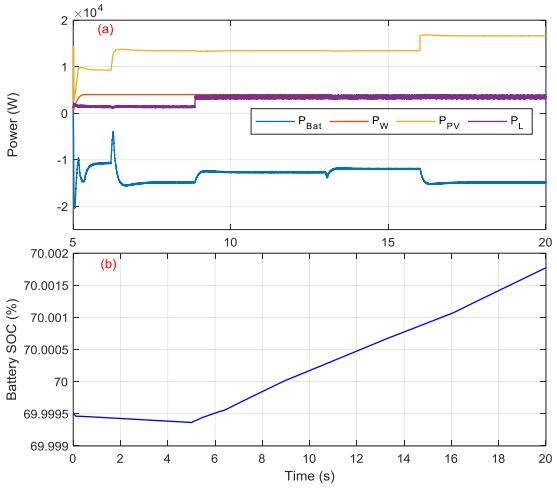

FIGURE 35. Results analysis of HRES power and battery SOC during PI control method with upper SOC limit and PV MPPT (a) Power- exchange among PV, wind, battery, and load (b) Battery SOC upper limit during charging mode.

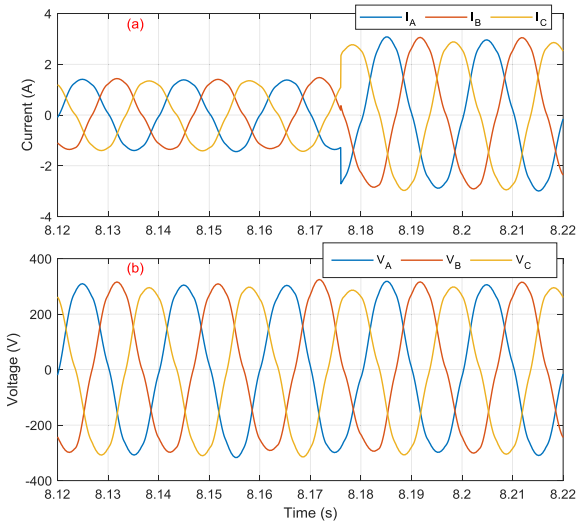

FIGURE 36. Three-phase load signals during PI control method with lower SOC limit and PV MPPT (a) Three-phase ac current (b)Three-phase ac voltage.

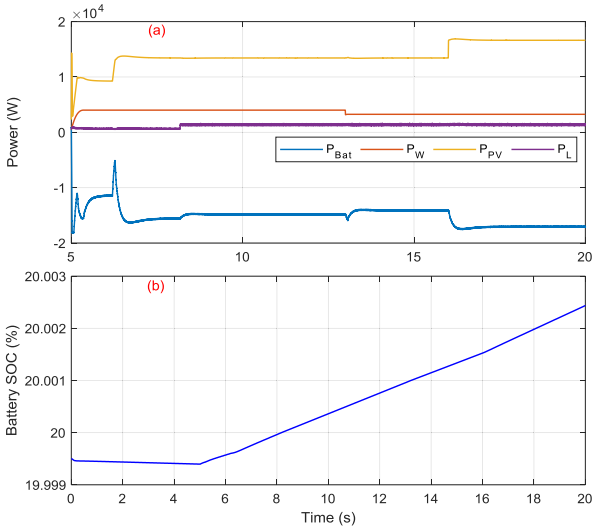

FIGURE 37. Analysis of HRES Power and battery SOC during PI control method with lower SOC limit and PV MPPT (a) Power- exchange among PV, wind, battery, and load (b) Battery SOC lower limit during charging mode.

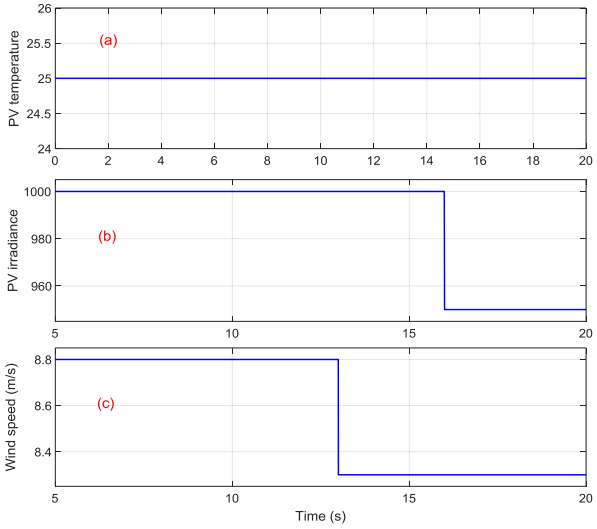

FIGURE 38. Input signals of solar and WT during FCS-MPC operation using upper SOC limit without PV MPPT (a) PV temperature (b) Variable PV irradiance (c) Variable wind speed.

Further, the more load power ripples are observed in the case of PI control (see Fig. 42) as compared to the efficient load power profile as shown in Fig. 39 which shows better performance of the FCS-MPVC strategy.

7) POWER OSCILLATIONS

To investigate the load power ripples in specific, Fig 43 shows the comparison of load powers obtained by PI and FCS-MPVC strategies. From 5-10 s, the power ripples magnitude with PI control is 482 W and this magnitude increases to 1000 W from 10-20 s; while the power ripple magnitude in case of FCS-MPVC strategy is only 30 W which is summarized in Table 10. Increasing load demand will inject more power ripples which are evident from the higher load curve.

8) THD ANALYSIS (FCS-MPC CONTROL)

Fig 44 and Fig 45 are analyzed in MATLAB/Simulink to test the proposed model in terms of THD for both currents as well as a voltage with and without PV-MPPT. Fig 44 shows the THD analysis (0.66 %) of HRES with PV-MPPT for three-phase load voltage and current respectively. While Fig 45 shows the THD analysis (0.30 %) of HRES without PV-MPPT for both current and voltage respectively.

Fewer THD values (0.30 %) in a case when no PV-MPPT is implemented show that the PV-MPPT boost controller also contributes more harmonics. THD of 5.44 % is observed in PI-based models which are higher as compared to FCS-MPVC approaches.

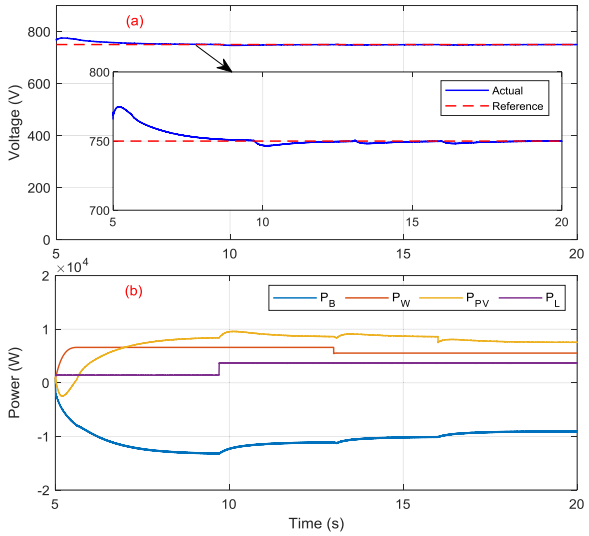

FIGURE 39. Voltage and power signals during FCS-MPC operation using upper SOC limit without PV MPPT (a) A dc voltage regulation under fluctuating source and variable load (b) Power- exchange among PV, wind, battery, and load.

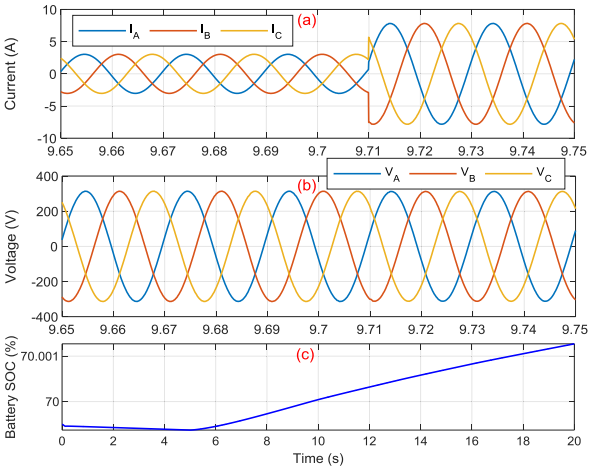

FIGURE 40. Analysis of output signals with battery SOC during FCS-MPC operation using upper SOC limit without PV MPPT (a) Three-phase ac current (b) Three-phase ac voltage (c) Battery SOC upper limit during charging mode.

9) THD ANALYSIS (PI CONTROL)

Fig. 46 and Fig. 47 are analyzed in MATLAB/Simulink to analyze the proposed model for harmonic analysis (THD) for both currents as well as voltage signals with and without PV-MPPT. Fig 46 shows the THD analysis (5.46 %) of HRES with PV-MPPT for three-phase load voltage and current respectively. While Fig 47 shows the THD analysis (5.44 %) of HRES without PV-MPPT for both voltage and current signals respectively. Fewer THD values (5.44 %) in a case when no PV-MPPT is implemented show that the PV-MPPT boost controller also contributes towards harmonics. THD of 5.44 % of PI-based models which are higher as compared to the suggested FCS-MPC model.

It is pertinent to mention here that the PI controllers' parameters are manually tuned, and no optimization

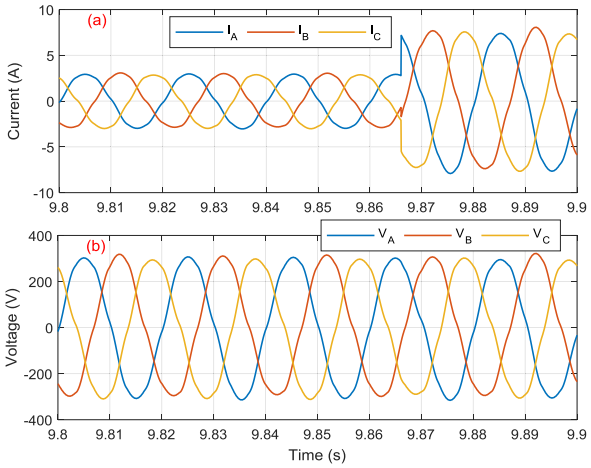

FIGURE 41. Load signals during PI control operation using upper SOC limit without PV MPPT (a) Three-phase ac current (b)Three-phase load voltage.

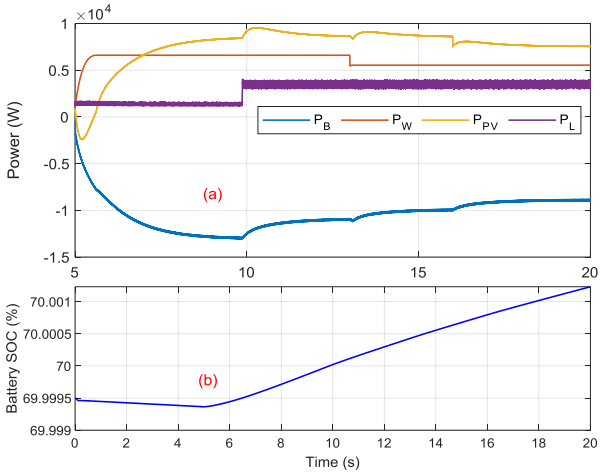

FIGURE 42. Signal analysis of Power and battery SOC during PI control operation using upper SOC limit without PV MPPT (a) Power- exchange among PV, wind, battery, and load (b) Battery SOC.

technique is applied. Before achieving the optimal results, the effect of K_p and K_i on system response and stability of the system for various combinations of K_p and K_i are tested by trial and error method. It was observed that a proportional controller (K_p) reduces the rise time as well as a steady-state error but has no guaranty to completely eliminate the steady-state error. While an integral controller (K_i) completely eliminates the steady-state error but has worsened the transient response. So, a lot of efforts are being made to find the trade-off between the two parameters to keep tracking the reference values of dc-link voltage and renewables' power.

VII. SUGGESTED SCHEME FEATURES AND COMPARATIVE ANALYSIS WITH LITERATURE

Table 10 shows the comparison of design optimization costs between the suggested HRES in Pakistan and HRES plans implemented worldwide. Based on component sizing and capital investments, the NPC values are implicitly not equal for the suggested HRESs. However, COE is an alternative

TABLE 10. Comparative analysis between suggested optimal HRES model with literature studies.

Ref	Region	HRES Plan	NPC ($)	COE ($/kWh)
[51]	India	PV-WT-DG-BESS-Converter	517277	0.458
[25]	Nigeria	PV-WT-DG-BESS-Converter	2370131	0.700
[40]	Iraq	PV-DG-BESS-Converter	138,704	0.264
[40]	Iraq	PV-DG-BESS-Converter	115,722	0.220
[40]	Iraq	PV-DG-BESS-Converter	110,191	0.210
[29]	India	PV-Biogas-Hydro-BESS-Converter	813000	-
[30]	Ethiopia	PV-WT	-	0.350
[83]	Turkey	PV-WT-FC-Converter	607,298	1.306
[53]	Bangladesh	PV-WT-DG-BESS-Converter	200,000	0.500
[84]	Pakistan	PV-Hydro-DG-BESS-Converter	40407000	0.175
[33]	Malaysia	PV-DG-BESS-Converter	970,368	0.194
[85]	Nigeria	PV-WT-DG-BESS-Converter	379,914	0.487
[54]	Nigeria	Grid-PV-BESS-Converter	302,543	1.247
[86]	Saudi Arabia	PV-WT-DG-BESS-Converter	8,130,000	0.164
[87]	Iran	PV-WT-BESS-Converter	676,345	0.274
[42]	Pakistan	WT-DG-BESS-Converter	14,846	0.309
[2]	India	PV-WT-BESS-Converter	228,353	0.288
[25]	Nigeria	PV-DG-BESS-Converter	2,225,387	0.658
[28]	China	WT-BESS-Converter	-	0.187
[43]	Canada	PV-WT-BGG-BESS-Converter	41,900,000	0.385
[44]	Egypt	PV-WT-DG-BESS-Converter	1,684,118	0.190
[49]	Iraq	PV-Hydro-DG-BESS-Converter	92381	0.0458
[10]	Morocco	PV-DG-BESS-Converter	10,195.56	0.570
Current study	**Pakistan**	PV-WT-DG-BESS-Converter	28,620	0.311

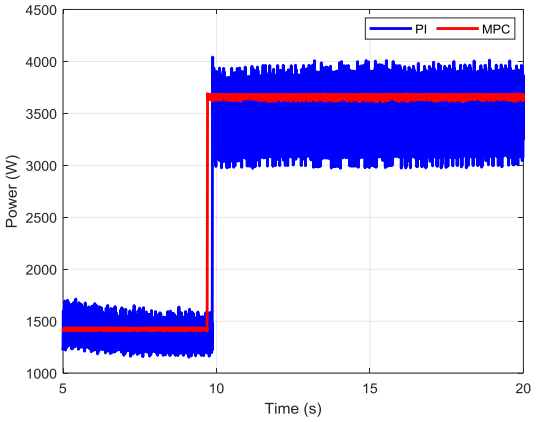

FIGURE 43. Comparison of load power oscillations for PI and MPC signals during PV MPPT operation.

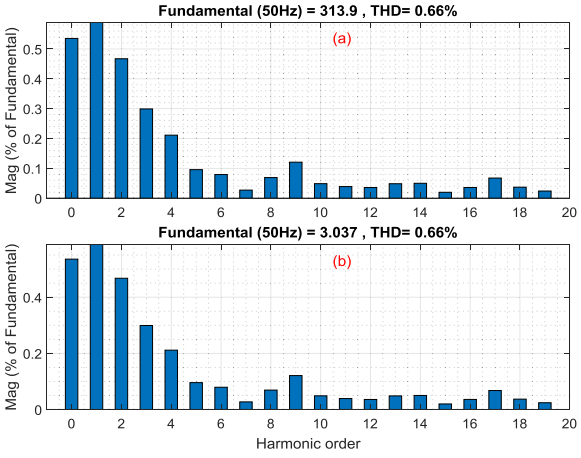

FIGURE 44. THD Analysis with FCS-MPC using PV-MPPT scheme (a) Three-phase load voltage (b) Three-phase load current.

comparison tool as an important metric for the cost of renewable generated power. India, Malaysia, and Pakistan have the lowest COE as compared to other countries. While COE in Turkey and Nigeria are the highest. In Pakistan, HRES with hydro is studied while wind integration is investigated in the current study. Based on the obtained results in this paper, the comparison also highlights fair agreement with other studies and presents insight into the economic feasibility of HRES in Pakistan. Although the table shows two case studies of Pakistan by suggesting HRES models, the incorporation of wind generation and the proposed HRES model for the selected area are not investigated in any research literature so far.

The comparison of THD between proposed work and the literature is shown in Table 11. THD values of 0.30% for the current study are lower than that of the system presented in Ref. [38]. Wind-battery-converter system which is presented in Ref. [42] has lower THD but the integration of PV is not incorporated in that system. Table 12 shows the comparison of THD and load power ripples between PI and FCS-MPVC controllers. Low THD and power ripples of FCS-MPVC based management strategy outperform the strategy based on

TABLE 11. Suggested FCS-MPC against PI.

Ref	Study System	Fundamental Voltage	Fundamental Voltage mismatch (%)	THD (%)	
				Voltage	Current
[38]	PV-Wind-Battery-Converter	326.7	5.05	1.83	2.67
[42]	Wind-Battery-Converter	308.7	0.75	0.26	-
Current study	PV-Wind-Battery-Converter	314.9	0.93	0.30	0.30

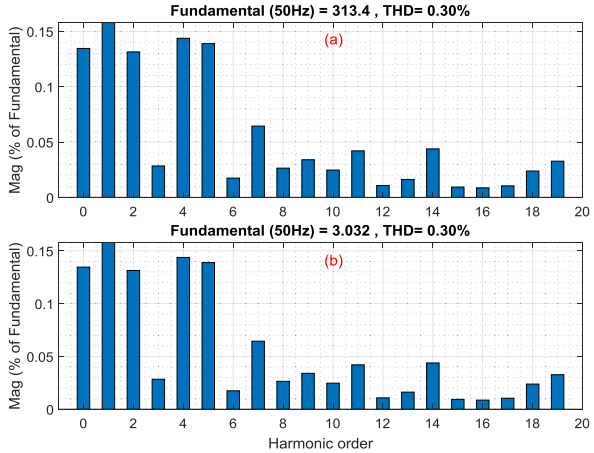

FIGURE 45. THD Analysis with FCS-MPC without using PV-MPPT scheme (a) Three-phase load voltage (b) Three-phase load current.

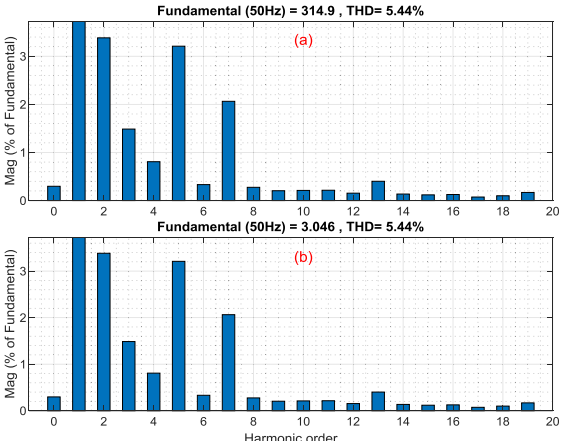

FIGURE 47. THD Analysis with PI control without using PV-MPPT (a) Three-phase load voltage (b) Three-phase load current.

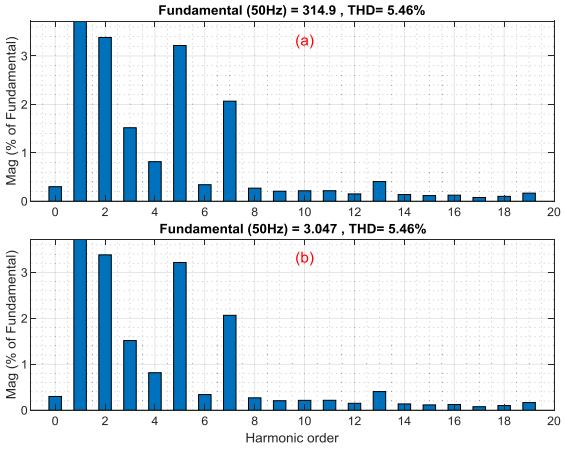

FIGURE 46. THD Analysis with PI control using PV-MPPT scheme (a) Three-phase load voltage (b) Three-phase load current.

TABLE 12. Performance analysis for the suggested EMS against PI.

Methodology	THD (%)	Load Power Ripples
PI	5.44	±480W (5s-10s) ±1000W (10s-20s)
Proposed FCS-MPVC	0.30	±30W (5s-20s)

PI control. It is pertinent to mention here that the significant decrease in THD value during proposed FCS-MPC methodology for a particular application can be verified from the output voltage/current signals for example the difference between Fig 32 and Fig 34 etc.

The main concluding remarks of the presented study is summarized below:

- The feasible configuration scheme with PV-wind-diesel-BSS-converter is achieved with the minimum NPC ($ 28,620) and COE ($ 0.311/kWh). Therefore, 100 % renewable energy generation penetration is ensured, along with no supply shortage.
- The cost of energy is observed high ($ 0.318/kWh) during diesel operation (case-2). It is therefore analyzed that DG plays a critical role in carbon emission for off-grid residential HRES.
- The NPC of the suggested system is five times less ($ 28,620) than the base scheme ($ 156,037). Hence, off-grid operation with diesel alone is not recommended, which is normally used in Pakistan.
- Zero carbon emission and fuel intake are observed for the suggested feasible winning plan while 11,965 kg/yr and 4,571 L/yr for the base case respectively.
- Promising results are observed during verification of the proposed EMS under fluctuating PV irradiance/temperature, and wind speed with abrupt load variations.
- The power quality is improved for an islanded (standalone) HRES by using FCS-MPC.
- Compared to conventional control strategy, the suggested FCS-MPC strategy is more robust towards transient response (less rise and fall time) during a fluctuating voltage supply at the dc bus.
- The reference voltage is fully tracked by the system voltage with no steady-state error while the stability of HRES operation with 0.30 % THD for load voltage is ensured which is below 5 % according to

the regulations of the IEEE standard 929, 2000 and IEEE-519 standards [2].

- Better power quality is obtained with voltage regulation under steady-state and transient modes by using applied management and control scheme.
- Energy management with SOC is also comprehensively examined during fluctuating generation and variable load conditions.
- The design of PI controllers is presented by trial and error method to get maximum solar and wind power under-regulated dc bus voltage.
- An incremental conductance (IC) algorithm is applied for maximum power extraction as a conventional method reported in the literature.
- The performance of reconfigurable inverter during generation fluctuation and variable loads is validated through simulations.
- The HRES model which is proposed in this paper will be helpful for government and energy sector planners to execute suitable policies and mechanism by integrating more renewable generation for a reliable, economical, and environment-friendly HRES scenarios. This research outcome will also open the new purview for model designers, hybrid microgrid (MG) planners, and researchers to effectively and efficiently design and utilize the HRERs by keeping in view the intermittent generation profile to handle increasing, unpredictable and abrupt load demand of the society of this global world.

VIII. CONCLUSION

Standalone HRES with PV-wind-battery is proposed as the optimal and economically most viable system, as determined by techno-economic studies carried out through HOMER and MATLAB along with FCS-MPC of a reconfigurable inverter, to fulfill the residential electricity requirement of Sherani district in the Province of Baluchistan, Pakistan. Firstly, optimal sizing of HRES components and economic investigation is performed through HOMER, while simulation studies for the suggested area with practical and real data of load profile as well as weather is investigated using different costs (capital, replacement, O&M), operating life, and efficiencies of HRES components, project lifetime, meteorological data assessment, and interest rate as the input parameters; load demand, resources availability, operating reserves, allowable capacity shortage, GHG emission penalties as optimization constraints; and NPC as decision variable. Out of nine possible optimal configurations namely PV-wind-battery, PV-wind-diesel-battery, PV-battery, PV-diesel-battery, wind-diesel-battery, PV-wind-diesel, PV-diesel, wind-diesel, and diesel-battery, as examined during this work, PV-wind-battery is obtained as the most feasible and economically viable configuration (i.e. winning plan) with minimum NPC ($ 28,620) and COE ($ 0.311/kWh) which shows 81.65 % reduction in cost and 100% preserving in toxic emission, while fulfilling 100 % energy demand with 67.3 % of excess energy. The proposed optimal HRES design (winning plan) comprises 13.4 kW PV, 4 kW wind, 3.88 kW converter, and 20 units of 2.37 kWh lead-acid battery.

Optimal sizes of HRES components are then used to design a management and control strategy in MATLAB/Simulink with finite control set model predictive control (FCS-MPC) of reconfigurable inverter for technical analysis based on power balance between HRES elements, constant dc and ac voltages, safe operating range of battery SOC, efficient ac voltage quality, during variations of PV irradiance, wind speed, as well as load demand. The results are validated through simulations with total harmonic distortion (THD) of 0.30 % which is well below the allowable limit according to IEEE-929 and IEEE-519 standards as compared to 5.44 % THD with the conventional PI control scheme.

The presented scheme would be an assessing tool for the governments, energy sector/microgrid planners, model designers, and researchers to investigate suitable policies, mechanisms, effective and efficient design of HRESs. An increasing, unpredictable and abrupt load demand of the society can be handled by integrating more renewable generation in terms of a reliable, economical, and environment-friendly scenarios with an understanding of intermittent generation profile. The future work includes microgrid reconfiguration under inverter and rectification mode to control the voltage and frequency during the standalone mode, and power flow during the grid-connected mode.

ACKNOWLEDGMENT

This work was supported by the Architecture and Urban Development Research Program funded by the Ministry of Land, Infrastructure, and Transport of the Korean government under Grant 19AUDP-B099686-02.

REFERENCES

[1] E. Muh and F. Tabet, "Comparative analysis of hybrid renewable energy systems for off-grid applications in Southern Cameroons," *Renew. Energy*, vol. 135, pp. 41–54, May 2019.

[2] O. Krishan and S. Suhag, "Techno-economic analysis of a hybrid renewable energy system for an energy poor rural community," *J. Energy Storage*, vol. 23, pp. 305–319, Jun. 2019.

[3] J. Kumari, P. Subathra, J. E. Moses, and D. Shruthi, "Economic analysis of hybrid energy system for rural electrification using HOMER," in *Proc. Int. Conf. Innov. Elect., Electron., Instrum. Media Technol. (ICEEIMT)*, Feb. 2017, pp. 151–156.

[4] W. Ullah, S. Noor, and A. Tariq, "The development of a basic framework for the sustainability of residential buildings in Pakistan," *Sustain. Cities Soc.*, vol. 40, pp. 365–371, Jul. 2018.

[5] *Greenhouse Gas (GHG) Emissions*. Accessed: Dec. 14, 2019. [Online]. Available: https://www.epa.gov/ghgemissions

[6] X. Kong, X. Liu, L. Ma, and K. Y. Lee, "Hierarchical distributed model predictive control of standalone wind/solar/battery power system," *IEEE Trans. Syst., Man, Cybern., Syst.*, vol. 49, no. 8, pp. 1570–1581, Aug. 2019.

[7] M. Mehreganfar, M. H. Saeedinia, S. A. Davari, C. Garcia, and J. Rodriguez, "Sensorless predictive control of AFE rectifier with robust adaptive inductance estimation," *IEEE Trans. Ind. Informat.*, vol. 15, no. 6, pp. 3420–3431, Jun. 2019.

[8] F. Salem and M. I. Mosaad, "A comparison between MPC and optimal PID controllers: Case studies," in *Proc. Michael Faraday IET Int. Summit*, Sep. 2015, pp. 59–65.

[9] S. Odhano, P. Zanchetta, M. Tang, and C. A. Silva, "MPC using modulated optimal voltage vector for voltage source inverter with LC output filter," in *Proc. IEEE Energy Convers. Congr. Expo. (ECCE)*, Sep. 2018, pp. 6865–6871.
[10] S. M. Shaahid, L. M. Alhems, and M. K. Rahman, "Techno-economic assessment of establishment of wind farms in different provinces of Saudi Arabia to mitigate future energy challenges," *Therm. Sci.*, vol. 23, no. 5, pp. 2909–2918, 2019.
[11] H. A. Khan, H. F. Ahmad, M. Nasir, M. F. Nadeem, and N. A. Zaffar, "Decentralised electric power delivery for rural electrification in Pakistan," *Energy Policy*, vol. 120, pp. 312–323, Sep. 2018.
[12] *Wind Energy Projects in Pakistan*. Accessed: Aug. 25, 2019. [Online]. Available: http://www.pmd.gov.pk/wind/Wind_Project_files/Page351.html
[13] M. H. Nawaz, M. U. Khan, A. Zahra, M. Ali, R. Wazir, and K. Ullah, "Optimal economic analysis of hybrid off grid (standalone) energy system for provincial capitals of Pakistan : A comparative study based on simulated results using real-time data," in *Proc. Int. Conf. Power Gener. Syst. Renew. Energy Technol. (PGSRET)*, Sep. 2018.
[14] *National Power Policy of Pakistan*. Accessed: Aug. 25, 2019. [Online]. Available: https://www-pub.iaea.org/MTCD/Publications/PDF/cnpp2018/countryprofiles/Pakistan/Pakistan.htm
[15] A. L. Bukar and C. W. Tan, "A review on stand-alone photovoltaic-wind energy system with fuel cell: System optimization and energy management strategy," *J. Cleaner Prod.*, vol. 221, pp. 73–88, Jun. 2019.
[16] F. S. F. Appavou, A. Brown, B. Epp, D. Gibb, B. Kondev, A. McCrone, H. E. Murdock, E. Musolino, L. Ranalder, J. L. Sawin, K. Seyboth, and J. Skeen, "Renewables in cities global status report," Frankfurt School-UNEP Centre/BNEF, Global Trends Renew. Energy Investment, Tech. Rep., 2018. [Online]. Available: http://www.fs-unep-centre.org
[17] A. Yahiaoui, K. Benmansour, and M. Tadjine, "Control, analysis and optimization of hybrid PV-diesel-battery systems for isolated rural city in Algeria," *Sol. Energy*, vol. 137, pp. 1–10, Nov. 2016.
[18] J. Li, W. Wei, and J. Xiang, "A simple sizing algorithm for stand-alone PV/wind/battery hybrid microgrids," *Energies*, vol. 5, no. 12, pp. 5307–5323, Dec. 2012.
[19] F. Diab, H. Lan, L. Zhang, and S. Ali, "An environmentally-friendly tourist village in Egypt based on a hybrid renewable energy system—Part one: What is the optimum city?" *Energies*, vol. 8, no. 7, pp. 6926–6944, Jul. 2015.
[20] F. Diab, H. Lan, L. Zhang, and S. Ali, "An environmentally-friendly tourist village in Egypt based on a hybrid renewable energy system–Part two: A net zero energy tourist village," *Energies*, vol. 8, no. 7, pp. 6945–6961, Jul. 2015.
[21] J.-H. Cho, M.-G. Chun, and W.-P. Hong, "Structure optimization of stand-alone renewable power systems based on multi object function," *Energies*, vol. 9, no. 8, p. 649, Aug. 2016.
[22] J. Lu, W. Wang, Y. Zhang, and S. Cheng, "Multi-objective optimal design of stand-alone hybrid energy system using entropy weight method based on HOMER," *Energies*, vol. 10, no. 10, p. 1664, Oct. 2017.
[23] N. Priyadarshi, S. Padmanaban, D. M. Ionel, L. Mihet-Popa, and F. Azam, "Hybrid PV-Wind, micro-grid development using quasi-Z-source inverter modeling and control-experimental investigation," *Energies*, vol. 11, no. 9, 2018.
[24] J. Faria, J. Pombo, M. Calado, and S. Mariano, "Power management control strategy based on artificial neural networks for standalone PV applications with a hybrid energy storage system," *Energies*, vol. 12, no. 5, p. 902, Mar. 2019.
[25] S. O. Oyedepo, T. Uwoghiren, P. O. Babalola, S. C. Nwanya, O. Kilanko, R. O. Leramo, A. K. Aworinde, T. Adekeye, J. A. Oyebanji, and O. A. Abidakun, "Assessment of decentralized electricity production from hybrid renewable energy sources for sustainable energy development in Nigeria," *Open Eng.*, vol. 9, no. 1, pp. 72–89, Mar. 2019.
[26] N. Priyadarshi, V. Ramachandaramurthy, S. Padmanaban, and F. Azam, "An ant colony optimized MPPT for standalone hybrid PV-wind power system with single Cuk converter," *Energies*, vol. 12, no. 1, p. 167, Jan. 2019.
[27] C. Mekontso, A. Abubakar, S. Madugu, O. Ibrahim, and Y. A. Adediran, "Review of optimization techniques for sizing renewable energy systems," *Comput. Eng. Appl. J.*, vol. 8, no. 1, pp. 13–30, Feb. 2019.
[28] T. Ma and M. S. Javed, "Integrated sizing of hybrid PV-wind-battery system for remote island considering the saturation of each renewable energy resource," *Energy Convers. Manage.*, vol. 182, pp. 178–190, Feb. 2019.
[29] M. Das, M. A. K. Singh, and A. Biswas, "Techno-economic optimization of an off-grid hybrid renewable energy system using metaheuristic optimization approaches–case of a radio transmitter station in India," *Energy Convers. Manage.*, vol. 185, pp. 339–352, Apr. 2019.
[30] R. Samikannu, V. Sampath Kumar, B. Diarra, and R. Ravi, "Cost optimization and development of hybrid energy systems for rural areas in ethiopia with a balance of their energy need and resources availability (A case study–on Tuludimtu)," *J. Test. Eval.*, vol. 47, no. 6, Nov. 2019, Art. no. 20180462.
[31] P. Das and D. K. Mahanta, "Feasibility analysis of standalone solar-wind hybrid energy system in Guwahati," *AIP Conf. Proc.*, vol. 2091, no. 1, 2019, Art. no. 020010.
[32] J. Carroquino, J.-L. Bernal-Agustín, and R. Dufo-López, "Standalone renewable energy and hydrogen in an agricultural context: A demonstrative case," *Sustainability*, vol. 11, no. 4, p. 951, Feb. 2019.
[33] E.-T. Chok, Y. S. Lim, and K. H. Chua, "Novel fuzzy-based control strategy for standalone power systems for minimum cost of electricity in rural areas," *Sustain. Energy Technol. Assessments*, vol. 31, pp. 199–211, Feb. 2019.
[34] R. Muthukumar and P. Balamurugan, "A model predictive controller for improvement in power quality from a hybrid renewable energy system," *Soft Comput.*, vol. 23, no. 8, pp. 2627–2635, Apr. 2019.
[35] B. S. Sami, N. Sihem, B. Zafar, C. Adnane, and A. E. Ahmed, "Performance evaluation of an appraisal autonomous system with hydrogen energy storage devoted for tunisian remote housing," in *Proc. Int. Conf. Smart Innov., Syst. Technol.*, 2019, pp. 274–281.
[36] X. Luo, J. Liu, Y. Liu, and X. Liu, "Bi-level optimization of design, operation, and subsidies for standalone solar/diesel multi-generation energy systems," *Sustain. Cities Soc.*, vol. 48, Jul. 2019, Art. no. 101592.
[37] S. Abdul-Wahab, Y. Charabi, A. M. Al-Mahruqi, I. Osman, and S. Osman, "Selection of the best solar photovoltaic (PV) for Oman," *Sol. Energy*, vol. 188, pp. 1156–1168, Aug. 2019.
[38] P. S. Sikder and N. Pal, "Modeling of an intelligent battery controller for standalone solar-wind hybrid distributed generation system," *J. King Saud Univ., Eng. Sci.*, to be published.
[39] W. Jing, C. H. Lai, D. K. Ling, W. S. Wong, and M. D. Wong, "Battery lifetime enhancement via smart hybrid energy storage plug-in module in standalone photovoltaic power system," *J. Energy Storage*, vol. 21, pp. 586–598, Feb. 2019.
[40] A. Aziz, M. Tajuddin, M. Adzman, M. Ramli, and S. Mekhilef, "Energy management and optimization of a PV/diesel/battery hybrid energy system using a combined dispatch strategy," *Sustainability*, vol. 11, no. 3, p. 683, Jan. 2019.
[41] M. Guezgouz, J. Jurasz, and B. Bekkouche, "Techno-economic and environmental analysis of a hybrid PV-WT-PSH/BB standalone system supplying various loads," *Energies*, vol. 12, no. 3, p. 514, Feb. 2019.
[42] H. U. R. Habib, S. Wang, M. R. Elkadeem, and M. F. Elmorshedy, "Design optimization and model predictive control of a standalone hybrid renewable energy system: A case study on a small residential load in Pakistan," *IEEE Access*, vol. 7, pp. 117369–117390, 2019.
[43] M. Bagheri, S. H. Delbari, M. Pakzadmanesh, and C. A. Kennedy, "City-integrated renewable energy design for low-carbon and climate-resilient communities," *Appl. Energy*, vol. 239, pp. 1212–1225, Apr. 2019.
[44] F. Diab, H. Lan, L. Zhang, and S. Ali, "An environmentally friendly factory in Egypt based on hybrid photovoltaic/wind/diesel/battery system," *J. Cleaner Prod.*, vol. 112, pp. 3884–3894, Jan. 2016.
[45] E. Diemuodeke, A. Addo, C. Oko, Y. Mulugetta, and M. Ojapah, "Optimal mapping of hybrid renewable energy systems for locations using multi-criteria decision-making algorithm," *Renew. Energy*, vol. 134, pp. 461–477, Apr. 2019.
[46] K. Murugaperumal, P. Ajay, and D. V. Raj, "Energy storage based MG connected system for optimal management of energy: An ANFMDA technique," *Int. J. Hydrogen Energy*, vol. 44, no. 16, pp. 7996–8010, Mar. 2019.
[47] F. Fodhil, A. Hamidat, and O. Nadjemi, "Potential, optimization and sensitivity analysis of photovoltaic-diesel-battery hybrid energy system for rural electrification in Algeria," *Energy*, vol. 169, pp. 613–624, Feb. 2019.
[48] M. Jahangiri, A. Haghani, A. Alidadi Shamsabadi, A. Mostafaeipour, and L. M. Pomares, "Feasibility study on the provision of electricity and hydrogen for domestic purposes in the south of Iran using grid-connected renewable energy plants," *Energy Strategy Rev.*, vol. 23, pp. 23–32, Jan. 2019.
[49] A. S. Aziz, M. F. N. Tajuddin, M. R. Adzman, A. Azmi, and M. A. Ramli, "Optimization and sensitivity analysis of standalone hybrid energy systems for rural electrification: A case study of Iraq," *Renew. Energy*, vol. 138, pp. 775–792, Aug. 2019.

[50] C. Y. Acevedo-Arenas, A. Correcher, C. Sánchez-Díaz, E. Ariza, D. Alfonso-Solar, C. Vargas-Salgado, and J. F. Petit-Suárez, "MPC for optimal dispatch of an AC-linked hybrid PV/wind/biomass/H_2 system incorporating demand response," *Energy Convers. Manage.*, vol. 186, pp. 241–257, Apr. 2019.
[51] V. Sohoni, S. Gupta, and R. K. Nema, "Design of wind-PV based hybrid standalone energy systems for three sites in central India," *Trans. Elect. Eng. Electron. Commun.*, vol. 17, no. 1, pp. 24–34, 2019.
[52] B. Belabbas, T. Allaoui, M. Tadjine, and M. Denai, "Power management and control strategies for off-grid hybrid power systems with renewable energies and storage," *Energy Syst.*, vol. 10, no. 2, pp. 355–384, May 2019.
[53] M. Jobayer, S. M. Salimullah, S. Datta, T. Rahman, and M. S. Alam, "Standalone hybrid minigrid for empowering every families in rural areas without dependency to grid electricity," in *Proc. Int. Conf. Sustain. Comput. Sci., Technol. Manage.*, 2019, pp. 589–593.
[54] A. J. Babalola, A. D, Yakubu, "Development of an alternative hybrid power system using hybrid micro power optimization model (HOMER)," *Int. J. Adv. Ind. Eng.*, vol. 7, no. 1, pp. 1–9, 2019.
[55] S. Vadi, S. Padmanaban, R. Bayindir, F. Blaabjerg, and L. Mihet-Popa, "A review on optimization and control methods used to provide transient stability in microgrids," *Energies*, vol. 12, no. 18, p. 3582, Sep. 2019.
[56] *An Introduction to Pakistan*. Accessed: Aug. 25, 2019. [Online]. Available: http://pakhumanitarianforum.org/
[57] *Introduction to Pakistan*. Accessed: Aug. 25, 2019. [Online]. Available: https://www.slideshare.net/
[58] *Introduction to Pakistan*. Accessed: Aug. 25, 2019. [Online]. Available: http://www.geographia.com/indx04.htm
[59] M. Kamran, "Current status and future success of renewable energy in Pakistan," *Renew. Sustain. Energy Rev.*, vol. 82, pp. 609–617, Feb. 2018.
[60] A. Ashfaq and A. Ianakiev, "Features of fully integrated renewable energy atlas for Pakistan; wind, solar and cooling," *Renew. Sustain. Energy Rev.*, vol. 97, pp. 14–27, Dec. 2018.
[61] *Wind System Installation*. Accessed: Dec. 7, 2019. [Online]. Available: https://www.windenergy.com
[62] *Encyclopaedia Britanica, Geographical Map of Pakistan, 2005*. Accessed: Dec. 7, 2019. [Online]. Available: https://www.britannica.com/place/Pakistan
[63] *Global Wind Altlas*. Accessed: Dec. 7, 2019. [Online]. Available: https://globalwindatlas.info/
[64] *Global Solar Atlas*. Accessed: Dec. 14, 2019. [Online]. Available: https://globalwindatlas.info/
[65] M. A. Husain, A. Tariq, S. Hameed, M. S. B. Arif, and A. Jain, "Comparative assessment of maximum power point tracking procedures for photovoltaic systems," *Green Energy Environ.*, vol. 2, no. 1, pp. 5–17, Jan. 2017.
[66] S. Ebrahimi, M. Jahangiri, H. A. Raiesi, and A. R. Ariae, "Optimal planning of on-grid hybrid microgrid for remote island using HOMER software, Kish in Iran," *Int. J. Energy* vol. 3, no. 2, pp. 13–21, 2018.
[67] A. Tani, M. B. Camara, and B. Dakyo, "Energy management in the decentralized generation systems based on renewable energy-ultracapacitors and battery to compensate the wind/load power fluctuations," *IEEE Trans. Ind. Appl.*, vol. 51, no. 2, pp. 1817–1827, Mar. 2015.
[68] A. C. Duman and Ö. Güler, "Techno-economic analysis of off-grid PV/wind/fuel cell hybrid system combinations with a comparison of regularly and seasonally occupied households," *Sustain. Cities Soc.*, vol. 42, pp. 107–126, Oct. 2018.
[69] A. M. Aly, A. M. Kassem, K. Sayed, and I. Aboelhassan, "Design of microgrid with flywheel energy storage system using HOMER software for case study," in *Proc. Int. Conf. Innov. Trends Comput. Eng. (ITCE)*, Feb. 2019, pp. 485–491.
[70] J. Hu, Y. Xu, K. W. Cheng, and J. M. Guerrero, "A model predictive control strategy of PV-battery microgrid under variable power generations and load conditions," *Appl. Energy*, vol. 221, pp. 195–203, Jul. 2018.
[71] N. Bizon, "Effective mitigation of the load pulses by controlling the battery/SMES hybrid energy storage system," *Appl. Energy*, vol. 229, pp. 459–473, Nov. 2018.
[72] F. K. Abo-Elyousr and A. Elnozahy, "Bi-objective economic feasibility of hybrid micro-grid systems with multiple fuel options for islanded areas in Egypt," *Renew. Energy*, vol. 128, pp. 37–56, Dec. 2018.
[73] S. Sinha and S. Chandel, "Review of software tools for hybrid renewable energy systems," *Renew. Sustain. Energy Rev.*, vol. 32, pp. 192–205, Apr. 2014.
[74] M. D. A. B. Rozmi, G. S. Thirunavukkarasu, E. Jamei, M. Seyedmahmoudian, S. Mekhilef, A. Stojcevski, and B. Horan, "Role of immersive visualization tools in renewable energy system development," *Renew. Sustain. Energy Rev.*, vol. 115, Nov. 2019, Art. no. 109363.
[75] A. Mills, "Simulation of hydrogen-based hybrid systems using Hybrid2," *Int. J. Hydrogen Energy*, vol. 29, no. 10, pp. 991–999, Aug. 2004.
[76] Y. Pan, L. Liu, T. Zhu, T. Zhang, and J. Zhang, "Feasibility analysis on distributed energy system of Chongming County based on RETScreen software," *Energy*, vol. 130, pp. 298–306, Jul. 2017.
[77] G. Zubi, R. Dufo-López, G. Pasaoglu, and N. Pardo, "Techno-economic assessment of an off-grid PV system for developing regions to provide electricity for basic domestic needs: A 2020–2040 scenario," *Appl. Energy*, vol. 176, pp. 309–319, Aug. 2016.
[78] M. S. Saleem, N. Abas, A. R. Kalair, S. Rauf, A. Haider, M. S. Tahir, and M. Sagir, "Design and optimization of hybrid solar-hydrogen generation system using TRNSYS," *Int. J. Hydrogen Energy*, to be published.
[79] S. Ferrari, F. Zagarella, P. Caputo, and M. Bonomolo, "Assessment of tools for urban energy planning," *Energy*, vol. 176, pp. 544–551, Jun. 2019.
[80] C. Bastholm and F. Fiedler, "Techno-economic study of the impact of blackouts on the viability of connecting an off-grid PV-diesel hybrid system in Tanzania to the national power grid," *Energy Convers. Manage.*, vol. 171, pp. 647–658, Sep. 2018.
[81] R. Lingamuthu and R. Mariappan, "Power flow control of grid connected hybrid renewable energy system using hybrid controller with pumped storage," *Int. J. Hydrogen Energy*, vol. 44, no. 7, pp. 3790–3802, Feb. 2019.
[82] Y. Sawle, S. Gupta, and A. K. Bohre, "Socio-techno-economic design of hybrid renewable energy system using optimization techniques," *Renew. Energy*, vol. 119, pp. 459–472, Apr. 2018.
[83] B. Dursun and E. Aykut, "An investigation on wind/PV/fuel cell/battery hybrid renewable energy system for nursing home in Istanbul," *Proc. Inst. Mech. Eng. A, J. Power Energy*, vol. 233, no. 5, pp. 616–625, Aug. 2019.
[84] H. R. Habib and T. Mahmood, "Optimal planning and design of hybrid energy system for UET Taxila," in *Proc. Int. Conf. Electr. Eng. (ICEE)*, Mar. 2017, pp. 1–9.
[85] I. Sofimieari, M. W. B. Mustafa, and F. Obite, "Modelling and analysis of a PV/wind/diesel hybrid standalone microgrid for rural electrification in Nigeria," *Bull. Elect. Eng. Inform.*, vol. 8, no. 4, pp. 1468–1477, 2019.
[86] A. B. Awan, "Performance analysis and optimization of a hybrid renewable energy system for sustainable NEOM city in Saudi Arabia," *J. Renew. Sustain. Energy*, vol. 11, no. 2, Mar. 2019, Art. no. 025905.
[87] S. Ashrafi Goudarzi, F. Fazelpour, G. B. Gharehpetian, and M. A. Rosen, "Techno-economic assessment of hybrid renewable resources for a residential building in tehran," *Environ. Prog Sustain. Energy*, vol. 38, no. 5, Sep. 2019, Art. no. 13209.

ESSAM A. AL-AMMAR (Senior Member, IEEE) received the M.S. degree from the University of Alabama, Tuscaloosa, AL, USA, in 2003, and the Ph.D. degree from Arizona State University, in 2007. He worked as a Power/Software Engineer with Lucent Technologies, Riyadh, for two years. He is currently an Associate Professor with the Electrical Engineering Department, King Saud University, Riyadh, Saudi Arabia. He was the Governor's Advisor in Electricity Co-Generation Regulatory Authority (ECRA). Also, he was an Advisor with the Ministry of Water and Electricity (MOWE) and a former Energy Consultant for Riyadh Techno Valley (RTV). He involved in many local and international committees in different aspects in the area of power and electrical energy. He published nearly 100 articles and 20 patents in energy and water. His current interests include high voltage engineering, power system transmission and distribution, and renewable energy and smart grid. He is a Senior Member Saudi Engineering Committee since 1997.

HABIB UR RAHMAN HABIB received the B.Sc. degree in electrical engineering and the M.Sc. degree in electrical power engineering from the University of Engineering and Technology Taxila, Pakistan, in 2009 and 2015, respectively. He is currently pursuing the Ph.D. degree with the State Key Laboratory of Advanced Electromagnetic Engineering and Technology, Huazhong University of Science and Technology, Wuhan, China. Since 2009, he has been with the COMSATS Institute of Information Technology, Pakistan, and the Wah Engineering College, University of Wah, Pakistan. He has been a Management Trainee Officer with the Maintenance Department, Dynamic Packaging Pvt., Ltd., Lahore, Pakistan. He is also with the Department of Electrical Engineering, University of Engineering and Technology Taxila, Pakistan. His research interests include electrical planning and estimation, energy resources and planning, modeling and simulation, renewable energy technology and management, smart grid applications in power systems, distributed generation and microgrid, power electronics, power quality, artificial intelligence, fuzzy controllers, algorithm design, and optimization, model predictive control, and its application in power industry.

KOTB M. KOTB received the B.Sc. and M.Sc. degrees in electrical engineering from Tanta University, Egypt, in 2012 and 2017, respectively. He is currently pursuing the Ph.D. degree with the Budapest University of Technology and Economics, Budapest, Hungary. He has been started working as a Teaching Assistant with the Department of Electrical Power and Machines Engineering, Faculty of Engineering, Tanta University, since 2013. In May 2017, he has been promoted as an Assistant Lecturer with the Department of Electrical Power and Machines Engineering. His research topics are directed to power electronics, renewable energy systems, and microgrid technologies.

SHAORONG WANG received the B.Sc. degree in electrical engineering from Zhejiang University, Hangzhou, China, in 1984, the M.Sc. degree in electrical engineering from North China Electric Power University, China, in 1990, and the Ph.D. degree from the Huazhong University of Science and Technology, China, in 2004. He is currently a Professor with the School of Electrical and Electronics Engineering, Huazhong University of Science and Technology. His research interests include smart grid, power system planning, and big data of power systems.

WONSUK KO received the B.S. and M.S. degrees from Kyungwon University, Seongnam, South Korea, in 1996 and 1998, respectively, and the Ph.D. degree in electrical engineering from the University of Central Florida, Orlando, FL, USA, in 2007. He was a Researcher with the Gachon Energy Research Institute, Gachon University, South Korea, where he was also an Instructor with the Department of Electrical Engineering. He is currently an Assistant Professor of electrical engineering with King Saud University. His research interests include electromagnetic modeling, magnetic levitation, energy management, and smart grid.

MAHMOUD F. ELMORSHEDY (Student Member, IEEE) was born in Gharbeya, Egypt, in 1989. He received the B.Sc. and M.Sc. degrees in electrical engineering from Tanta University, Egypt, in 2012 and 2016, respectively. He is currently pursuing the Ph.D. degree with the State Key Laboratory of Advanced Electromagnetic Engineering and Technology, Huazhong University of Science and Technology, China. He has been started working as a Teaching Assistant with the Department of Electrical Power and Machines Engineering, Faculty of Engineering, Tanta University, since 2013. In June 2016, he was promoted as an Assistant Lecturer with the Department of Electrical Power and Machines Engineering. His research interests include linear induction motor, predictive control, power electronics, and renewable energy.

ASAD WAQAR received the degree in electrical engineering from UET Taxila, in 2002, the master's degree in electrical power engineering from RWTH Aachen, Germany, in 2011, and the Ph.D. degree in electrical engineering from the Huazhong University of Science and Technology, China, in 2016. He is currently working as an Associate Professor with the Department of Electrical Engineering, Bahria University, Islamabad, Pakistan. His research interests include smart grids, microgrids operation and control, power quality, power electronics, energy economics, and network reinforcement planning.